PB82-197195

In-situ Aerodynamic Sizing of Aerosol Particles with the Spart Analyzer

Arkansas Univ. at Little Rock

Prepared for

Environmental Sciences Research Lab.
Research Triangle Park, NC

Apr 82

U.S. Department of Commerce
National Technical Information Service
NTIS

TECHNICAL REPORT DATA
(Please read Instructions on the reverse before completing)

1. REPORT NO.	2.	3. RECIPIENT'S ACCESSION NO.
EPA-600/3-82-009	Research report	PB82 197195

4. TITLE AND SUBTITLE	5. REPORT DATE
IN-SITU AERODYNAMIC SIZING OF AEROSOL PARTICLES WITH THE SPART ANALYZER	April 1982
	6. PERFORMING ORGANIZATION CODE

7. AUTHOR(S)	8. PERFORMING ORGANIZATION REPORT NO.
Malay K. Mazumder, R. E. Ware, J. D. Wilson, R. G. Renninger, P. C. McLeod and R. A. Sims	

9. PERFORMING ORGANIZATION NAME AND ADDRESS	10. PROGRAM ELEMENT NO.
University of Arkansas Little Rock, AR 72203	CDTA1D/01-0426 (FY-81)
	11. CONTRACT/GRANT NO.
	R804429

12. SPONSORING AGENCY NAME AND ADDRESS	13. TYPE OF REPORT AND PERIOD COVERED
Environmental Sciences Research Laboratory - RTP, NC Office of Research and Development U.S. Environmental Protection Agency Research Triangle Park, N. C. 27711	Final 6/76 - 2/80
	14. SPONSORING AGENCY CODE
	EPA/600/09

15. SUPPLEMENTARY NOTES

micrometer

16. ABSTRACT

A single particle aerodynamic relaxation time (SPART) analyzer has been developed to measure the aerodynamic size distribution of aerosol particulates in the range 0.1 to 10.0 μm in diameter. The analyzer sizes and counts individual suspended particles and droplets from sampled aerosols, determines their aerodynamic diameter, and generates the size distribution in real-time. The measurement is independent of the electrical and optical properties of the particles.

The size range and resolution of the SPART analyzer depend on the acoustic frequency. Operating at 27 kHz, the instrument's effective sampling rate was calibrated in the range of 0.3 to 6.0 μm using test aerosols containing monodisperse polystyrene latex spheres (PLS) and olive oil droplets. The instrument can count and size aerosol particulates at a maximum rate of 200 particles/sec. The sensing volume of the instrument is approximately 10^{-5} cc, which allows the size distribution measurement of an aerosol containing a relatively high particulate concentration without an appreciable coincidence loss.

.00001

17. KEY WORDS AND DOCUMENT ANALYSIS

a. DESCRIPTORS	b. IDENTIFIERS/OPEN ENDED TERMS	c. COSATI Field/Group

18. DISTRIBUTION STATEMENT	19. SECURITY CLASS (This Report)	21. NO. OF PAGES
RELEASE TO PUBLIC	UNCLASSIFIED	48
	20. SECURITY CLASS (This page)	22. PRICE
	UNCLASSIFIED	

EPA Form 2220-1 (Rev. 4-77) PREVIOUS EDITION IS OBSOLETE

BEGIN FIRST LINE OF TEXT HERE
CENTER OF PAGE
TOP OF IMAGE AREA

EPA-600/3-82-009
April 1982

PB82-197195

DROPPED HEAD; BEGIN SECTIONS HERE

IN-SITU AERODYNAMIC SIZING OF AEROSOL PARTICLES WITH THE SPART ANALYZER

by

M. K. Mazumder, R. E. Ware, J. D. Wilson,
R. G. Renninger, P. C. McLeod, and R. A. Sims
Department of Electronics and Instrumentation
University of Arkansas Graduate Institute of Technology
Little Rock, Arkansas 72203

6-1/2"
9-1/8"

Grant No. R 804429

Project Officer

Charles W. Lewis
Atmospheric Chemistry and Physics Division
Environmental Sciences Research Laboratory
Research Triangle Park, North Carolina 27711

ENVIRONMENTAL SCIENCES RESEARCH LABORATORY
OFFICE OF RESEARCH AND DEVELOPMENT
U.S. ENVIRONMENTAL PROTECTION AGENCY
RESEARCH TRIANGLE PARK, NORTH CAROLINA 27711

BEGIN LAST LINE OF TEXT
3/8"
BOTTOM OF IMAGE AREA; OUTSIDE DIMENSION FOR TABLES AND ILLUSTRATIONS

REPRODUCED BY
NATIONAL TECHNICAL INFORMATION SERVICE
U.S. DEPARTMENT OF COMMERCE
SPRINGFIELD, VA 22161

PAGE NUMBER

EPA Form 2350-4 (4-80)
(PREVIOUSLY CIN. EPA FORM 287)

☆ U.S. GOVERNMENT PRINTING OFFICE 1980-660-639

TYPING GUIDE SHEET

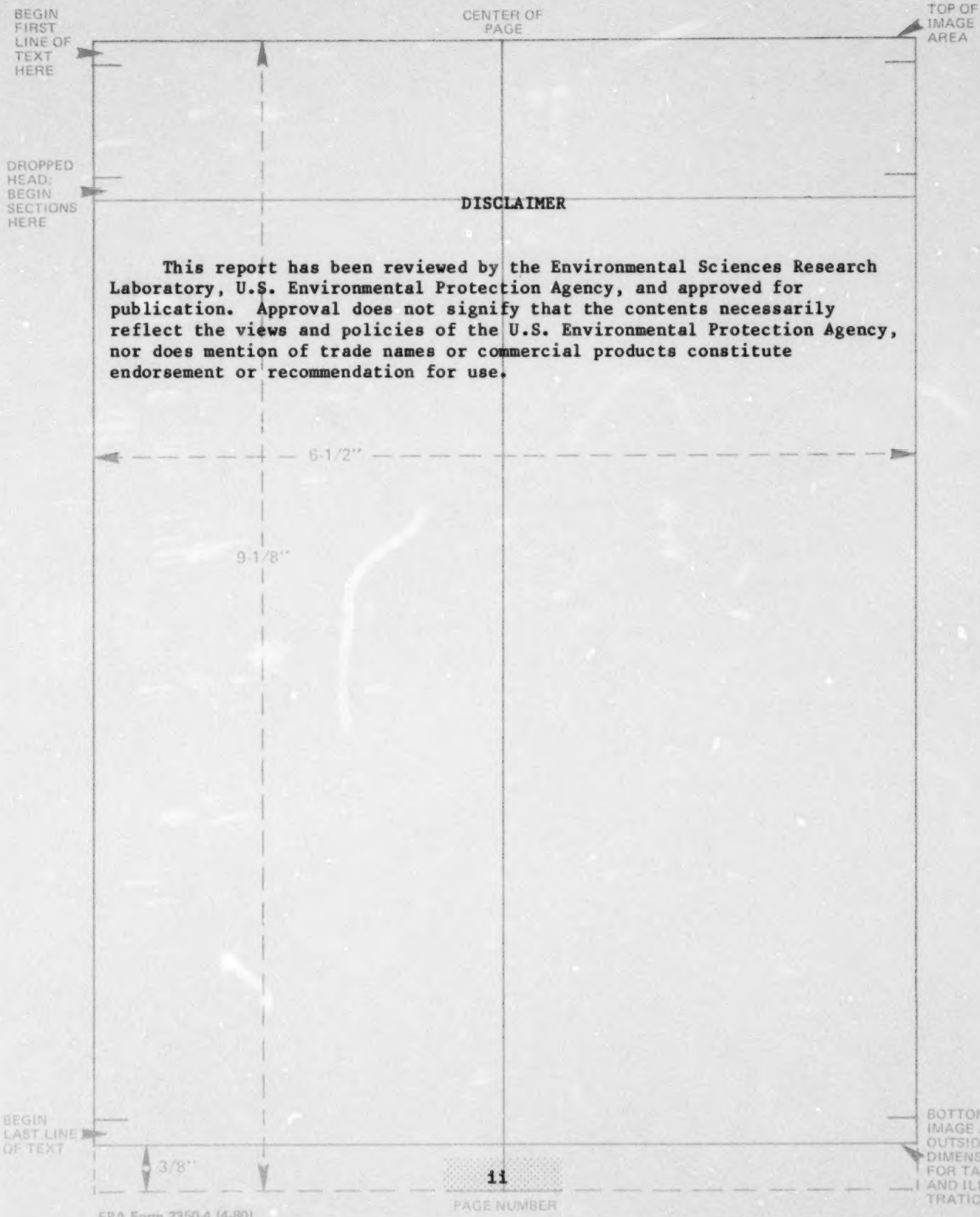

DISCLAIMER

This report has been reviewed by the Environmental Sciences Research Laboratory, U.S. Environmental Protection Agency, and approved for publication. Approval does not signify that the contents necessarily reflect the views and policies of the U.S. Environmental Protection Agency, nor does mention of trade names or commercial products constitute endorsement or recommendation for use.

EPA Form 2350-4 (4-80)
(PREVIOUSLY CIN. EPA FORM 287)

☆ U.S. GOVERNMENT PRINTING OFFICE 1980-660-639

TYPING GUIDE SHEET

BEGIN FIRST LINE OF TEXT HERE
CENTER OF PAGE
TOP OF IMAGE AREA
DROPPED HEAD; BEGIN SECTIONS HERE

ABSTRACT

A single particle aerodynamic relaxation time (SPART) analyzer has been developed to measure the aerodynamic size distribution of aerosol particulates in the range 0.1 to 10.0 μm in diameter. The analyzer sizes and counts individual suspended particles and droplets from sampled aerosols, determines their aerodynamic diameter, and generates the size distribution in real-time. The measurement is independent of the electrical and optical properties of the particles.

As each particle or droplet enters the sensing volume of the analyzer, it is subjected to acoustic oscillation of 27 kHz. Particle oscillation will lag acoustic excitation and this phase lag, ϕ, is related to the aerodynamic diameter d_a. The particle motion is detected by a laser Doppler velocimeter (LDV); a microphone monitors the acoustic field oscillation.

A microcomputer-based signal processor is programmed to compute d_a from ϕ for each particle count, assigning each one to its appropriate size channel. The stored data is available from memory via a digital printer in the following formats: (1) number of particles counted in each size channel vs. channel number, (2) the size distribution $dN/d(\log d_a)$, and (3) the volume distribution $dV/d(\log d_a)$.

The size range and resolution of the SPART analyzer depend on the acoustic frequency. Its effective sampling rate at 27 kHz was calibrated in the range of 0.3 to 6.0 μm using test aerosols containing monodisperse polystyrene latex spheres (PLS) and olive oil droplets. The instrument can count and size aerosol particulates at a maximum rate of 200 particles/sec. The sensing volume of the instrument is approximately 10^{-5} cc, which allows the size distribution measurement of an aerosol containing a relatively high particulate concentration without an appreciable coincidence loss.

This report was submitted in fulfillment of Grant No. R804429 by the Department of Electronics and Instrumentation, Graduate Institute of Technology, University of Arkansas, under the sponsorship of the U.S. Environmental Protection Agency. This report covers the period June 1, 1976, to February 29, 1980, and the work was completed as of February 29, 1980.

BEGIN LAST LINE OF TEXT
BOTTOM OF IMAGE AREA; OUTSIDE DIMENSION FOR TABLES AND ILLUSTRATIONS
3/8"

EPA Form 2350-4 (4-80)
(PREVIOUSLY CIN. EPA FORM 287)
☆ U.S. GOVERNMENT PRINTING OFFICE 1980-680-839
TYPING GUIDE SHEET

BEGIN FIRST LINE OF TEXT HERE
CENTER OF PAGE
TOP OF IMAGE AREA
DROPPED HEAD; BEGIN SECTIONS HERE

CONTENTS

Abstract iii

Figures vi

Tables viii

Acknowledgment ix

1. Introduction 1
2. Conclusions 3
3. Recommendations 4
4. Measurement of Aerodynamic Diameter 5
   - Motion of a Particle in an Acoustic Field 5
   - Measurement of d_a From Phase Lag (ϕ) 8
   - Measurement of d_a From Amplitude Ratio (V_p/U_g) 9
5. Description of the SPART Analyzer 12
   - Laser Doppler Velocimeter 12
   - Relaxation Cell 14
   - Signal Processing Circuit 16
   - Microcomputer-Based Data Processor 18
6. Resolution and Range 19
   - Relationship Between $\partial\phi/\partial(d_a)$ and d_a 19
   - Resolution of Δt Measurement 21
   - Size Range 22
7. Count Rate and Coincidence Loss 26
   - Effective Sampling Rate 26
   - Coincidence Error 28
8. Test Results 31
   - Calibration: Aerodynamic Size 31
   - Calibration: Aerosol Particulate Concentration 32
   - Measurement of Aerosol Size Distribution 33

References 36

Preceding page blank

BEGIN LAST LINE OF TEXT
BOTTOM OF IMAGE AREA; OUTSIDE DIMENSION FOR TABLES AND ILLUSTRATIONS
3/8"

PAGE NUMBER
EPA Form 2350-4 (4-80)
(PREVIOUSLY CIN/EPA FORM 287)
☆ U.S. GOVERNMENT PRINTING OFFICE 1980-860-639
TYPING GUIDE SHEET

BEGIN FIRST LINE OF TEXT HERE

CENTER OF PAGE

TOP OF IMAGE AREA

DROPPED HEAD: BEGIN SECTIONS HERE

FIGURES

Number		Page
1	Relationship between τ_p and d_a for air at STP.....	7
2	Calculated relationship between d_a and ϕ for different acoustic excitation frequencies.....	9
3	Ratio of the particle velocity (V_p/U_g) as a function of the frequency of excitation and the aerodynamic diameter.....	10
4	Computed values of V_p/U_g plotted as a function of time.....	11
5	Block diagram of the SPART analyzer	13
6	LDV beam geometry.....	14
7	Schematic of the inlet to the relaxation cell.....	15
8	Block diagram of the signal processing and data storage systems of the SPART analyzer.....	17
9	Acoustic excitation frequency for optimum size resolution as a function of d_a.....	20
10	Calculated value of the LDV sensing volume v_s plotted as a function of the laser beam intersection angle θ.....	27
11	Number distributions of aerosol particles containing a mixture of three sizes of PLS as measured by the SPART analyzer after calibration.....	31
12	Experimentally observed values of the effective sampling rate $Q(d_a)$ plotted as a function of d_a.....	33
13	Size distribution of atmospheric aerosol as determined by the SPART analyzer.....	34

BEGIN LAST LINE OF TEXT

BOTTOM OF IMAGE AREA; OUTSIDE DIMENSION FOR TABLES AND ILLUSTRATIONS

3/8"

PAGE NUMBER

EPA Form 2350-4 (4-80)

(PREVIOUSLY CIN. EPA FORM 267)

☆ U.S. GOVERNMENT PRINTING OFFICE 1980-680-639

TYPING GUIDE SHEET

BEGIN FIRST LINE OF TEXT HERE

CENTER OF PAGE

TOP OF IMAGE AREA

14 Growth of Bronkometer aerosol as measured by the SPART analyzer. The aerosol was generated by a metered-dose medical aerosol dispenser and was analyzed at 35 and 98 percent relative humidity while being maintained at 37°C..... 35

DROPPED HEAD; BEGIN SECTIONS HERE

6-1/2"

9-1/8"

BEGIN LAST LINE OF TEXT

3/8"

BOTTOM OF IMAGE AREA; OUTSIDE DIMENSION FOR TABLES AND ILLUSTRATIONS

EPA Form 2350-4 (4-80)

(PREVIOUSLY CIN, EPA FORM 287)

☆ U.S. GOVERNMENT PRINTING OFFICE 1980-680-639

TYPING GUIDE SHEET

BEGIN FIRST LINE OF TEXT HERE

CENTER OF PAGE

TOP OF IMAGE AREA

DROPPED HEAD; BEGIN SECTIONS HERE

TABLES

Number		Page
1	C_{ca}, τ_p, ϕ, Δt and n_c as a function of d_a for f= 27.0 kHz, f_s = 13.824 MHz.....	23
2	Channel Numbers vs Aerodynamic Diameters.....	24
3	Channel Numbers vs Aerodynamic Diameters.....	25
4	Effect of Coincidence Loss on the Size Distribution of Monodisperse 0.804 μm Polystyrene Latex Spheres as Measured by the SPART analyzer.....	30
5	Effect of Coincidence Loss on the Measured Size Distribution of Polydisperse DOS Aerosol as Measured by the SPART analyzer.....	30

BEGIN LAST LINE OF TEXT

BOTTOM OF IMAGE AREA; OUTSIDE DIMENSION FOR TABLES AND ILLUSTRATIONS

3/8"

PAGE NUMBER

EPA Form 2350-4 (4-80)
(PREVIOUSLY CIN, EPA FORM 287)

☆ U.S. GOVERNMENT PRINTING OFFICE 1980-660-639

TYPING GUIDE SHEET

BEGIN FIRST LINE OF TEXT HERE
CENTER OF PAGE
TOP OF IMAGE AREA
DROPPED HEAD; BEGIN SECTIONS HERE

ACKNOWLEDGMENT

The authors are indebted to the faculty, staff, and several students of the Department of Electronics and Instrumentation who worked on this project. The cooperative effort of the entire department working as a team made this project successful. Significant contributions were made by K. J. Kirsch, L. T. Sherwood, and A. Page in instrument development; R. W. Raible in designing electronic circuitry; and R. L. Bond and G. S. Ballard in optical system designs. The authors are thankful to W. Hood for computer programming, F. C. Hiller for his interest and contribution to the development of the instrument to study therapeutic aerosols, P. T. Archer for assistance in various phases of the project, L. Neidhardt for mechanical fabrication, and D. Watson, M. Elms and P. Roberson for editorial assistance.

The authors are grateful to the EPA project monitor, Dr. C. W. Lewis, whose continued interest, constructive criticism, and frequent review of progress helped significantly with development of the instrument.

The work was performed under the direction of the late Dr. M. K. Testerman, Professor and Head of the Department of Electronics and Instrumentation. He acted as the project manager and provided the leadership during the entire phase of this work.

BEGIN LAST LINE OF TEXT
3/8"
BOTTOM OF IMAGE AREA; OUTSIDE DIMENSION FOR TABLES AND ILLUSTRATIONS

EPA Form 2350-4 (4-80)
(PREVIOUSLY CIN. EPA FORM 287)
☆ U.S. GOVERNMENT PRINTING OFFICE 1980-660-639
TYPING GUIDE SHEET

BEGIN FIRST LINE OF TEXT HERE
CENTER OF PAGE
TOP OF IMAGE AREA
DROPPED HEAD; BEGIN SECTIONS HERE

SECTION 1

INTRODUCTION

The deposition of inhaled aerosol particulates within the lung depends primarily upon their aerodynamic diameter, defined as the diameter of a unit density spherical particle having the same aerodynamic properties as the particle in question. The site and quantity of lung deposition and, consequently, the possible health hazard resulting from inhaled particles can be determined from measurement of the aerodynamic size distribution of the aerosol. While there are numerous methods of sizing airborne particulates, none of the commercially available instruments can measure the aerodynamic diameter of individual, suspended particles and droplets in real time in the size range 0.1 to 10.0 μm in diameter. This size range contains the major mass fraction of respirable aerosols.

The geometric size distribution of particles can be measured by microscopic techniques. This method is tedious however and conversion of geometric size to aerodynamic diameter is difficult for nonspherical particles, and cannot be done even for spherical particles without knowledge of the particle's density. The optical diameters can be measured in real time by optical particle counters if the intensity of light scattered from particles of unknown geometrical size and refractive index is correlated with the optical diameter of a standard spherical particle of known optical properties. It is difficult to correlate the optical diameter to geometric and aerodynamic diameters.

Aerodynamic diameter can be determined by using a technique where the site of particle deposition is dependent upon the aerodynamic size. Cascade impactors are often used for analyzing aerodynamic size distributions. Although able to provide much useful information, various technical limitations impede their ability to determine the aerodynamic size distribution in many applications. Their limitations were reviewed by several workers.[1,2]

Any method requiring sample collection and subsequent analysis suffers the delay between deposition and measurement. Evaporation or condensation after collection may alter the mass, thereby altering the size distribution of the unstable particles. Measurements are required in real time when the size distribution of particulates changes with time because of condensation, evaporation, or coagulation, or when there are changes in the generation, sedimentation, or transportation processes. Real-time measurements are also necessary for efficient in-line monitoring of air filtration in devices where critical control adjustments are required.

BEGIN LAST LINE OF TEXT
BOTTOM OF IMAGE AREA OUTSIDE DIMENSION FOR TABLES AND ILLUSTRATIONS
3/8"

EPA Form 2350-4 (4-80)
(PREVIOUSLY CIN, EPA FORM 247)
☆ U.S. GOVERNMENT PRINTING OFFICE 1980-660-639

TYPING GUIDE SHEET

BEGIN FIRST LINE OF TEXT HERE
CENTER OF PAGE
TOP OF IMAGE AREA

The purpose of this study was to develop a laser-based instrument that can be used to monitor the size distribution of atmospheric aerosols within the respirable fraction, 0.1 to 10.0 μm in aerodynamic diameter. Measurements must be made in real time and on a single particle basis. The process of measurement must not be influenced by the properties of aerosols not related to size, such as refractive index, electrical charge, and chemical composition.

DROPPED HEAD; BEGIN SECTIONS HERE

The instrument developed under this study, a single particle aerodynamic relaxation time (SPART) analyzer, meets these criteria. The SPART analyzer sizes and counts individual particles from sampled aerosol, determines their aerodynamic diameters and generates the size distribution of the aerosol. Utilizing a frequency-biased differential laser Doppler velocimeter (LDV) and a microphone, the analyzer will determine the aerodynamic relaxation time τ_p of individual particles suspended in air. The quantity τ_p is the time in which a particle, when suspended in still air, reaches 63.2 percent of its terminal settling velocity. The aerodynamic diameter d_a is obtained from the value of τ_p. Thus, the measurement of size distribution can be made depending upon the aerodynamic properties of the particulates.

6-1/2"
9-1/8"
BEGIN LAST LINE OF TEXT
BOTTOM OF IMAGE AREA OUTSIDE DIMENSION FOR TABLES AND ILLUSTRATIONS
3/8"

PAGE NUMBER
EPA Form 2350-4 (4-80)
(PREVIOUSLY CIN, EPA FORM 237)
☆ U.S. GOVERNMENT PRINTING OFFICE 1980-660-639
TYPING GUIDE SHEET

BEGIN FIRST LINE OF TEXT HERE
CENTER OF PAGE
TOP OF IMAGE AREA
DROPPED HEAD; BEGIN SECTIONS HERE

SECTION 2

CONCLUSIONS

A new instrument has been develcped for measuring in real time the aerodynamic size distribution of aerosol particulates in the respirable range 0.1 to 10.0 μm in diameter. The instrument, a single particle aerodynamic relaxation time (SPART) analyzer, measures the aerodynamic relaxation time of individual particles and droplets without removing the particulates from their aerosol phase. Two prototype SPART analyzers, one for laboratory use and another for field applications, were developed under this study. Measurements can be made at a maximum count rate of 200 particles/sec, although coincidence error restricts the count rate to a lower limit. The size resolution is better than 0.1 μm in the range 0.3 to 3.0 μm in aerodynamic diameter. The size range and resolution depend upon the frequency of acoustic excitation used in the analyzer; the two prototype analyzers were operated at 27 kHz.

The SPART analyzer samples aerosol at a rate of 550 cc/min. Approximately 500 cc/min flows as sheath air. The effective sampling rate, the flow rate of the aerosol passing through the sensing volume, is approximately 0.6 cc/min for particles with aerodynamic diameters in the range of 0.3 to 6 μm. The effective sampling rate is reduced outside this range.

The SPART analyzer is currently used in several measuring applications: (1) the size distribution of atmospheric aerosols, (2) the size distribution of therapeutic aerosol at a temperature of 37° C and 98 percent relative humidity to simulate the ambient condition of the lung, and (3) the fractional efficiency of air pollution control devices as a function of aerodynamic diameter. Studies performed to date on the SPART analyzer indicate many potential uses for this instrument; however, several modifications and improvements are necessary before the instrument can receive routine usage.

BEGIN LAST LINE OF TEXT
3/8"
BOTTOM OF IMAGE AREA; OUTSIDE DIMENSION FOR TABLES AND ILLUSTRATIONS

EPA Form 2350-4 (4-80)
[PREVIOUSLY CIN. EPA FORM 267]
☆ U.S. GOVERNMENT PRINTING OFFICE 1980-680-539
TYPING GUIDE SHEET

BEGIN FIRST LINE OF TEXT HERE
CENTER OF PAGE
TOP OF IMAGE AREA
DROPPED HEAD: BEGIN SECTIONS HERE

SECTION 3

RECOMMENDATIONS

Research and development work during the project period has resulted in an instrument suitable for measuring the aerodynamic size distribution of aerosol particulates in the respirable range. Its unique feature of measuring the aerodynamic diameter of single-particles and droplets in real time, allows the SPART analyzer to complement other existing instruments used in measuring the size distribution of aerosols.

Although the prototype SPART analyzer has been operating satisfactorily for a period of approximately two years, many potential developments for its use have not been explored. Areas of potential development are: (1) increase of the range of the SPART analyzer to extend from 0.05 to 20.0 μm in aerodynamic diameter by operating the analyzer at two acoustic frequencies in sequential modes with improvement of the LDV optics and detection sensitivity; (2) increase of the effective sampling rate; (3) the automatic correction of the effective sampling rate as a function of aerodynamic diameter, (4) the modulation of the sensing volume so that smaller particles can be counted with a small sensing volume for a minimum coincidence loss while larger particles are counted with a large sensing volume for a high sampling rate; and (5) the modification of the SPART analyzer to measure both the effective shape factor and aerodynamic sizes of the particulates.

BEGIN LAST LINE OF TEXT
BOTTOM OF IMAGE AREA; OUTSIDE DIMENSION FOR TABLES AND ILLUSTRATIONS
3/8"

EPA Form 2350-4 (4-80)
(PREVIOUSLY CIN, EPA FORM 267)
☆ U.S. GOVERNMENT PRINTING OFFICE 1980-660-629
TYPING GUIDE SHEET

BEGIN FIRST LINE OF TEXT HERE
CENTER OF PAGE
TOP OF IMAGE AREA
DROPPED HEAD; BEGIN SECTIONS HERE

SECTION 4

MEASUREMENT OF AERODYNAMIC DIAMETER

MOTION OF A PARTICLE IN AN ACOUSTIC FIELD

A particle suspended in air will oscillate in an acoustic field. The amplitude and phase of oscillation will depend upon the aerodynamic relaxation time τ_p of the particle.[3] The relaxation time is the time during which the velocity of a particle moving with respect to a surrounding fluid medium declines by a factor of 1/e because of fluid resistance. The equation of motion of a particle of mass m_p can be written as

$$m_p(dv_p/dt) = F_{drag} - F_{ext}, \qquad (1)$$

where v_p is the velocity of the particle, F_{drag} is the drag force acting on the particle, and F_{ext} is the sum of the external forces on the particle. The external forces may be a combination of gravity, Brownian motion, electrostatic charges, thermophoresis, etc. If the Reynolds number of particle motion is less than 0.1, F_{drag} can be written from Stokes' Law[4] for a spherical particle of diameter d_p as

$$F_{drag} = -3\pi\eta d_p(v_p - u_g)/C_c, \qquad (2)$$

where η is the viscosity of the surrounding fluid medium, u_g is the fluid velocity, and C_c is the Cunningham correction factor for molecular slip. If F_{ext} is negligible, equation (1) can be written as

$$m_p(dv_p/dt) + 3\pi\eta d_p(v_p - u_g)/C_c = 0. \qquad (3)$$

If the fluid is subjected to an oscillatory motion caused by an acoustic excitation in a standing wave[5] of angular frequency ω, and amplitude U_g

$$u_g(t) = U_g \sin \omega t, \qquad (4)$$

equation (3) can be written as for $v_p(t)$, the motion of a suspended particle as a function of time,

$$(m_p C_c/3\pi\eta d_p)(dv_p/dt) + v_p = U_g \sin \omega t \qquad (5)$$

or $$\tau_p(dv_p/dt) + v_p = U_g \sin \omega t \qquad (6)$$

where $\tau_p = m_p Z$ is the relaxation time, and where

BEGIN LAST LINE OF TEXT
BOTTOM OF IMAGE AREA; OUTSIDE DIMENSION FOR TABLES AND ILLUSTRATIONS
3/8"

EPA Form 2350-4 (4-80)
(PREVIOUSLY CIN, EPA FORM 287)
© U.S. GOVERNMENT PRINTING OFFICE 1980-660-639
TYPING GUIDE SHEET

BEGIN FIRST LINE OF TEXT HERE
CENTER OF PAGE
TOP OF IMAGE AREA

$$Z = C_c/3\pi\eta d_p \qquad (7)$$

is the mechanical mobility of the particle. For a spherical particle,

$$\tau_p = \rho_p d_p^2 C_c/18\eta. \qquad (8)$$

DROPPED HEAD; BEGIN SECTIONS HERE

The dimensionless Cunningham correction factor C_c is unity for particles with diameters much larger than the mean free path, λ_g, of air molecules. For particles with diameters less than or comparable with λ_g (λ_g = 0.065 μm for air at STP), C_c can be written as

$$C_c = 1 + (2\lambda_g/d_p)[A + B \exp(-Cd_p/2\lambda_g)], \qquad (9)$$

where A = 1.257, B = 0.4, and C = 1.1, determined experimentally. For a nonspherical particle, d_p must be replaced by an equivalent diameter.

The motion of an individual particle $v_p(t)$ in the direction of motion of the acoustic wave can be written from the steady state solution of equation (6),

$$v_p(t) = [U_g/(1 + \omega^2\tau_p^2)^{1/2}]\sin(\omega t - \phi), \qquad (10)$$

where ϕ is the phase lag of the motion of a particle with respect to the motion of the element of air surrounding the particle undergoing acoustic excitation, and U_g is the amplitude of the fluid velocity. The quantity ϕ is related to τ_p by

$$\phi = \tan^{-1}(\omega\tau_p). \qquad (11)$$

For any particle, irrespective of its shape and density, τ_p can be written as

$$\tau_p = d_a^2 \rho_o C_{ca}/18\eta, \qquad (12)$$

where d_a is the aerodynamic diameter, ρ_o represents unit density, C_{ca} is the Cunningham molecular slip correction factor referred to d_a, and η is the viscosity of air. Figure 1 shows the relationship between τ_p and d_a for air at 20°C and at one atmospheric pressure. The Cunningham correction factor is strictly a function of the geometric diameter of a particle. But by regarding C_{ca} as a function of aerodynamic diameter[4], equations (11) and (12) can be combined to yield a unique relationship between ϕ and d_a, permitting the value of d_a to be determined from the measurement of ϕ.

BEGIN LAST LINE OF TEXT
BOTTOM OF IMAGE AREA; OUTSIDE DIMENSION FOR TABLES AND ILLUSTRATIONS
3/8"

EPA Form 2350-4 (4-80)
[PREVIOUSLY CIN. EPA FORM 287]
☆ U.S. GOVERNMENT PRINTING OFFICE 1980-660-639
TYPING GUIDE SHEET

BEGIN FIRST LINE OF TEXT HERE
CENTER OF PAGE
TOP OF IMAGE AREA
DROPPED HEAD; BEGIN SECTIONS HERE

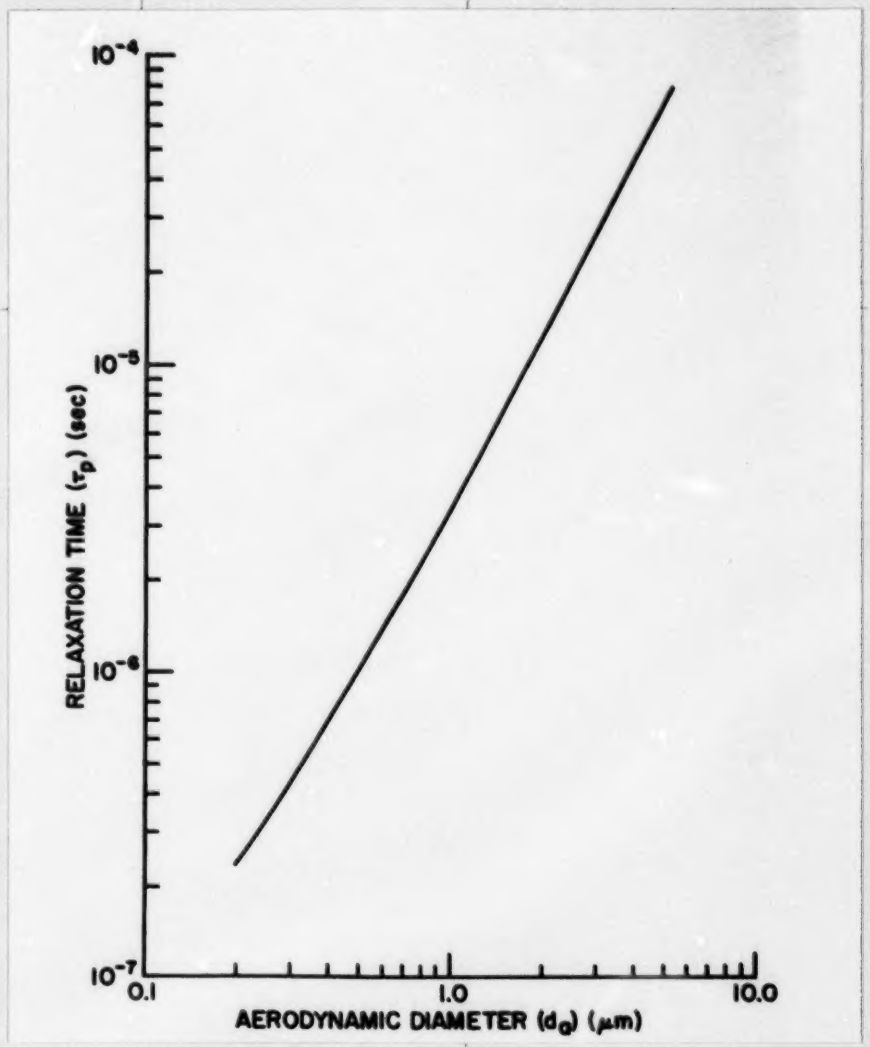

Figure 1. Relationship between τ_p and d_a for air at 20°C and at one atmospheric pressure.

BEGIN LAST LINE OF TEXT
BOTTOM OF IMAGE AREA; OUTSIDE DIMENSION FOR TABLES AND ILLUSTRATIONS
3/8"

EPA Form 2350-4 (4-80)
(PREVIOUSLY CIN. EPA FORM 287)
☆ U.S. GOVERNMENT PRINTING OFFICE 1980-660-639
TYPING GUIDE SHEET

BEGIN FIRST LINE OF TEXT HERE
CENTER OF PAGE
TOP OF IMAGE AREA
DROPPED HEAD; BEGIN SECTIONS HERE

MEASUREMENT OF d_a FROM PHASE LAG (ϕ)

The phase lag ϕ is related to τ_p by equation (11):

$$\tau_p = (1/\omega)\tan(\phi). \qquad (13)$$

From the value of τ_p, the product $d_a^2 C_{ca}$ can be determined from equation (12) because both ρ_o and η are known. If

$$d_a^2 C_{ca} \equiv X, \qquad (14)$$

then

$$X = 18\eta\tau_p/\rho_o. \qquad (15)$$

The quantity C_{ca} can be expressed as

$$C_{ca} = 1 + 2Y/d_a, \qquad (16)$$

from equation (9), where $Y = \lambda_g[1.257 + 0.4\exp(-1.1d_a/2\lambda_g)]$ and λ_g is the mean free path of air molecules. Combining equations (14) and (16) produces

$$X = d_a^2 + 2Yd_a. \qquad (17)$$

Solving for d_a results in

$$d_a = (Y^2 + X)^{1/2} - Y. \qquad (18)$$

The quantity X is known from measurements (equation 14), but Y is a function of d_a. Thus, an iterative algorithm is used to determine d_a. Assuming an initial value of Y_o as

$$Y_o = 1.257\lambda_g,$$

$$d_n = (Y_n^2 + X)^{1/2} - Y_n, \quad n = 0,1,2,\ldots, \qquad (19)$$

$$Y_{n+1} = \lambda_g[1.257 + 0.4\exp(-1.1d_n/2\lambda_g)]. \qquad (20)$$

The sequence $(d_n, n = 0,1,2,\ldots)$ converges rapidly to d_a.

Figure 2 shows the calculated relationship between d_a and ϕ for different frequencies of acoustic excitation. By suitably choosing two frequencies of excitation, e.g. 2.0 and 20.0 kHz, it is possible to measure d_a in the range 0.1 to 10.0 μm.

BEGIN LAST LINE OF TEXT
3/8"
BOTTOM OF IMAGE AREA; OUTSIDE DIMENSION FOR TABLES AND ILLUSTRATIONS

EPA Form 2350-4 (4-80)
(PREVIOUSLY CIN. EPA FORM 267)
☆ U.S. GOVERNMENT PRINTING OFFICE 1980-660-639
TYPING GUIDE SHEET

BEGIN FIRST LINE OF TEXT HERE
CENTER OF PAGE
TOP OF IMAGE AREA
DROPPED HEAD; BEGIN SECTIONS HERE

inertia of the particle plays a significant role and, as a result, the ratio of the amplitude of oscillation to that of the medium decreases. Eventually, if $\omega\tau_p$ assumes even larger values, a point is reached where the particles remain stationary in an acoustic field. Thus, for a given aerodynamic size, an intermediate frequency range of acoustic excitation exists in which the particles' relative amplitudes of oscillation can be used to determine the size of the particles. The calculated results based on equation (21) are shown in Figures 3 and 4, where the value of μ is plotted as a function of d_a for different values of acoustic excitation frequency (Figure 3), and as a function of time for different values of d_a (Figure 4).

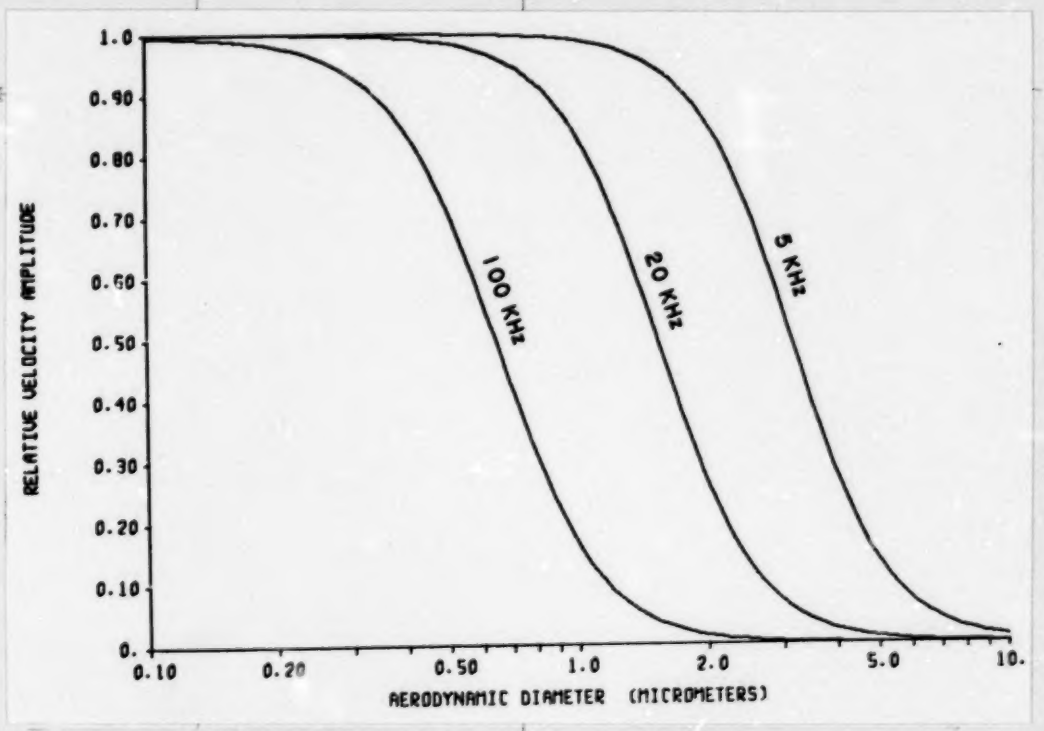

Figure 3. Ratio of the particle velocity (V_p/U_g) as a function of the frequency of excitation and the aerodynamic diameter.

BEGIN LAST LINE OF TEXT
BOTTOM OF IMAGE AREA; OUTSIDE DIMENSION FOR TABLES AND ILLUSTRATIONS
3/8"

EPA Form 2350-4 (4-80)
(PREVIOUSLY CIN, EPA FORM 287)
☆ U.S. GOVERNMENT PRINTING OFFICE 1980-660-539
TYPING GUIDE SHEET

BEGIN FIRST LINE OF TEXT HERE
CENTER OF PAGE
TOP OF IMAGE AREA
DROPPED HEAD; BEGIN SECTIONS HERE

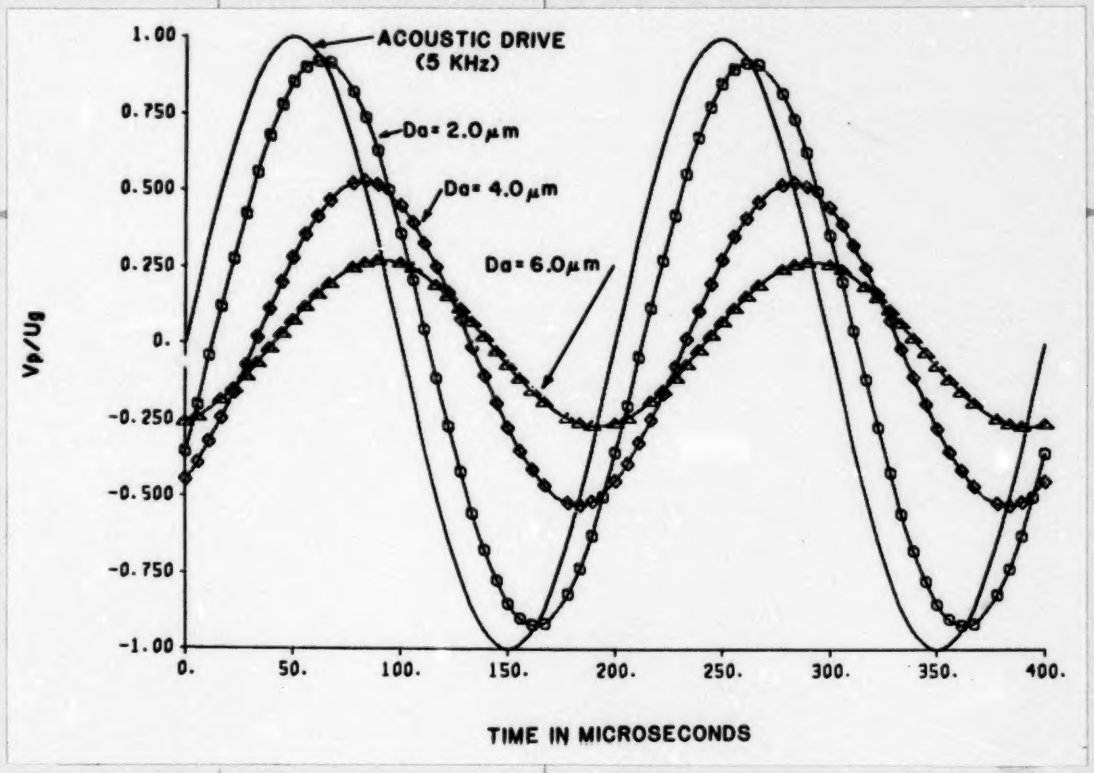

Figure 4. Computed values of V_p/U_g plotted as a function of time for different values of a_a.

BEGIN LAST LINE OF TEXT
3/8"
BOTTOM OF IMAGE AREA; OUTSIDE DIMENSION FOR TABLES AND ILLUSTRATIONS

EPA Form 2350-4 (4-80)
(PREVIOUSLY CIN. EPA FORM 287)
☆ U.S. GOVERNMENT PRINTING OFFICE 1980-660-639
TYPING GUIDE SHEET

BEGIN FIRST LINE OF TEXT HERE
CENTER OF PAGE
TOP OF IMAGE AREA
DROPPED HEAD; BEGIN SECTIONS HERE

SECTION 5

DESCRIPTION OF THE SPART ANALYZER

Two prototype SPART analyzers were constructed and tested for laboratory and field applications. The analyzers use a laser Doppler velocimeter (LDV) containing a sensing volume located at an antinode of an acoustic standing-wave pattern. The LDV measures $v_p(t)$ by detecting the Doppler shift of light scattered by an oscillating particle passing through the sensing volume; a microphone measures $u_g(t)$. The relative phase lag ϕ between $u_g(t)$ and $v_p(t)$ is calculated by a data-processing circuit. A microprocessor determines d_a as a function of ϕ. The process takes approximately 2.5 msec for each particle measurement.

LASER DOPPLER VELOCIMETER

Principles of the LDV are documented in current literature.[6] A frequency-shifted dual-beam LDV[7,8] is used in the SPART analyzer (Figure 5) to measure $v_p(t)$. The LDV transmission optics comprise an argon ion laser, a beam splitter, two Bragg cells, three mirrors, and a focusing lens. The receiving system of the LDV comprises a receiving lens, a pinhole, and a photomultiplier tube (PMT). Two frequency-shifted laser beams, focused by the transmission lens, intersect at a 20° angle forming an interference fringe pattern in the beam intersection. A portion of this fringe pattern is focused by the receiving optics creating the LDV sensing volume.

Assuming Gaussian beam intensity distributions, the focal point of the two intersecting beams will have a diameter of

$$d_f = (4/\pi)\lambda f/D_{(1/e^2)} \qquad (22)$$

where λ is the wavelength of laser radiation, f is the focal length of the lens, and $D_{(1/e^2)}$ is the Gaussian diameter of the laser beam incident on the lens. The probe volume can be described as an ellipsoid with semiaxes a, b, and c given by

$$2a = d_f/\cos(\theta/2)$$

$$2b = d_f/\sin(\theta/2)$$

BEGIN LAST LINE OF TEXT
BOTTOM OF IMAGE AREA OUTSIDE DIMENSION FOR TABLES AND ILLUSTRATIONS
3/8"

EPA Form 2350-4 (4-80)
(PREVIOUSLY CIN. EPA FORM 287)
☆ U.S. GOVERNMENT PRINTING OFFICE: 1980-680-839
TYPING GUIDE SHEET

BEGIN FIRST LINE OF TEXT HERE
CENTER OF PAGE
TOP OF IMAGE AREA
DROPPED HEAD; BEGIN SECTIONS HERE

$$2c = d_f$$

and the probe volume

$$v_s = (\pi/3)d_f^3/\sin(\theta) \qquad (23)$$

where θ is the angle of beam intersection. The fringe spacing is given by

$$d_i = \lambda/2\sin(\theta/2) \qquad (24)$$

and the number of fringes, n_f, within the probe volume is given by

$$n_f = 2a/d_i = [(8f\tan(\theta/2)]/D_{(1/e^2)} \qquad (25)$$

$$= (4/\pi)[S/D_{(1/e^2)}]$$

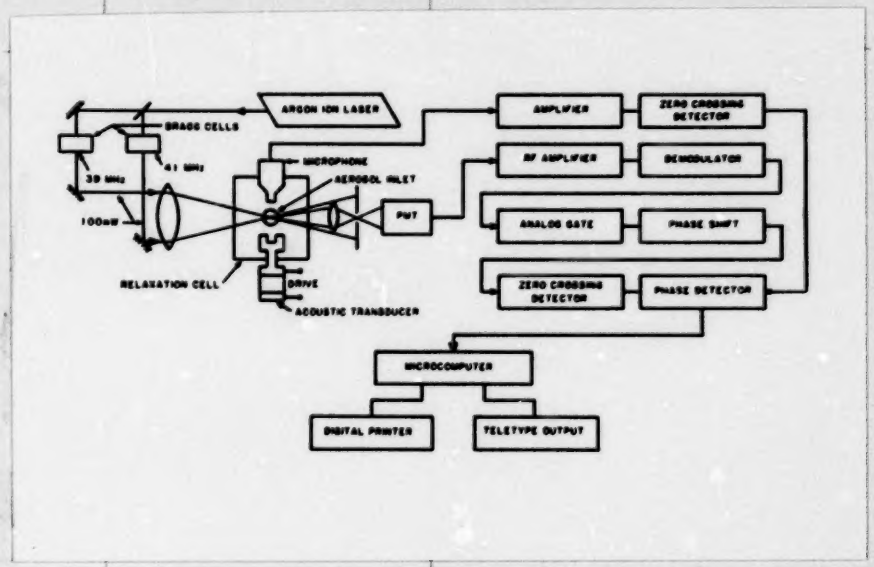

Figure 5. Block diagram of the SPART analyzer.

where S is the separation between the two incident laser beams at the secondary principal plane of the transmitting lens. The LDV probe volume and its effective cross sectional area are determined by the LDV beam geometry (Figure 6). The variation of the probe volume as a function of the angle θ and its significance on the performance of the SPART analyzer are discussed in section 7.

As each particle transits the sensing volume, the particle generates a Doppler signal burst. The duration of this burst is approximately 1 msec, which is the residence time of the particle inside the sensing volume. The

BEGIN LAST LINE OF TEXT
BOTTOM OF IMAGE AREA OUTSIDE DIMENSION FOR TABLE AND ILLUSTRATIONS
3/8"

EPA Form 2350-4 (4-80)
(PREVIOUSLY CIN. EPA FORM 287)
☆ U.S. GOVERNMENT PRINTING OFFICE 1980-660-639
TYPING GUIDE SHEET

BEGIN FIRST LINE OF TEXT HERE
CENTER OF PAGE
TOP OF IMAGE AREA
DROPPED HEAD: BEGIN SECTIONS HERE

instantaneous value of the Doppler shift f_D is given by

$$f_D = f_o + [2v_p(t)/\lambda]\sin(\theta/2), \qquad (26)$$

where f_o is the difference in frequency between the two Bragg-shifted laser beams and $v_p(t)$ is the particle velocity component normal to the fringe planes. Because v_p is a time-dependent quantity varying with an angular frequency $\omega(\omega = 2\pi f)$, the Doppler signal burst is an FM signal with a carrier frequency f_o (typically 2 MHz) and a modulating frequency f, which is the frequency of acoustic excitation that typically ranges from 2 to 50 kHz (Figure 2).

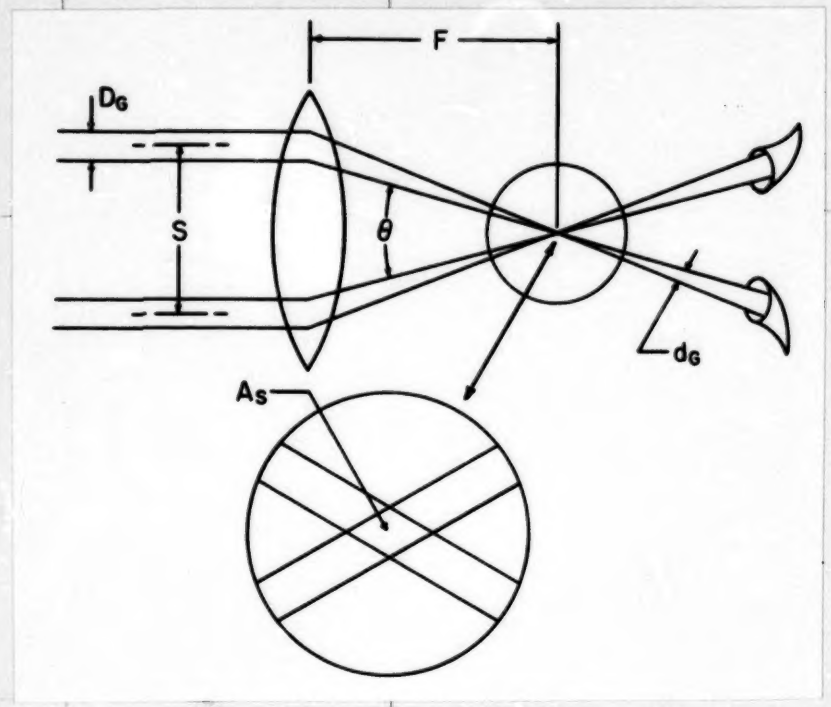

Figure 6. LDV beam geometry.

RELAXATION CELL

An aluminum chamber, frequently referred to as the relaxation cell, is used to provide a housing for the flow of the aerosol sample through the LDV sensing volume as well as the standing-wave pattern. The cell, with overall dimensions of 14.5 x 10.2 x 10.2 cm, has two optical windows on opposite sides for the transmission and receiving optics of the LDV, two aerosol sampling tubes, two acoustic transducers, and the LDV sensing volume located in the center. Figure 7 shows schematically the inlet of the relaxation cell.

BEGIN LAST LINE OF TEXT
BOTTOM OF IMAGE AREA, OUTSIDE DIMENSION FOR TABLES AND ILLUSTRATIONS
3/8"

EPA Form 2350-4 (4-80)
(PREVIOUSLY CIN. EPA FORM 287)
☆ U.S. GOVERNMENT PRINTING OFFICE 1980-660-639
TYPING GUIDE SHEET

BEGIN FIRST LINE OF TEXT HERE
CENTER OF PAGE
TOP OF IMAGE AREA
DROPPED HEAD; BEGIN SECTIONS HERE

portion of the aerosol sample, approximately 500 ml/min, is filtered and allowed to flow through the relaxation cell as sheath air leaving approximately 50 ml/min to flow across the LDV sensing volume. The effective sampling rate, Q, or the flow rate of aerosol actually transiting the LDV sensing volume, is approximately 0.6 ml/min. From the entrance into the relaxation cell, the aerosol flows vertically downward through the sampling tube. The tube is 8 cm long and has an inside diameter of 1.5 mm. The aerosol and the sheath air both exit through a 16-mm diameter tube. Internal loss of sample volume caused by wall deposition of the particles is minimal. The sampling and exit tubes share the same vertical axis, passing through the sensing volume, with a 1-cm separation between the tube ends.

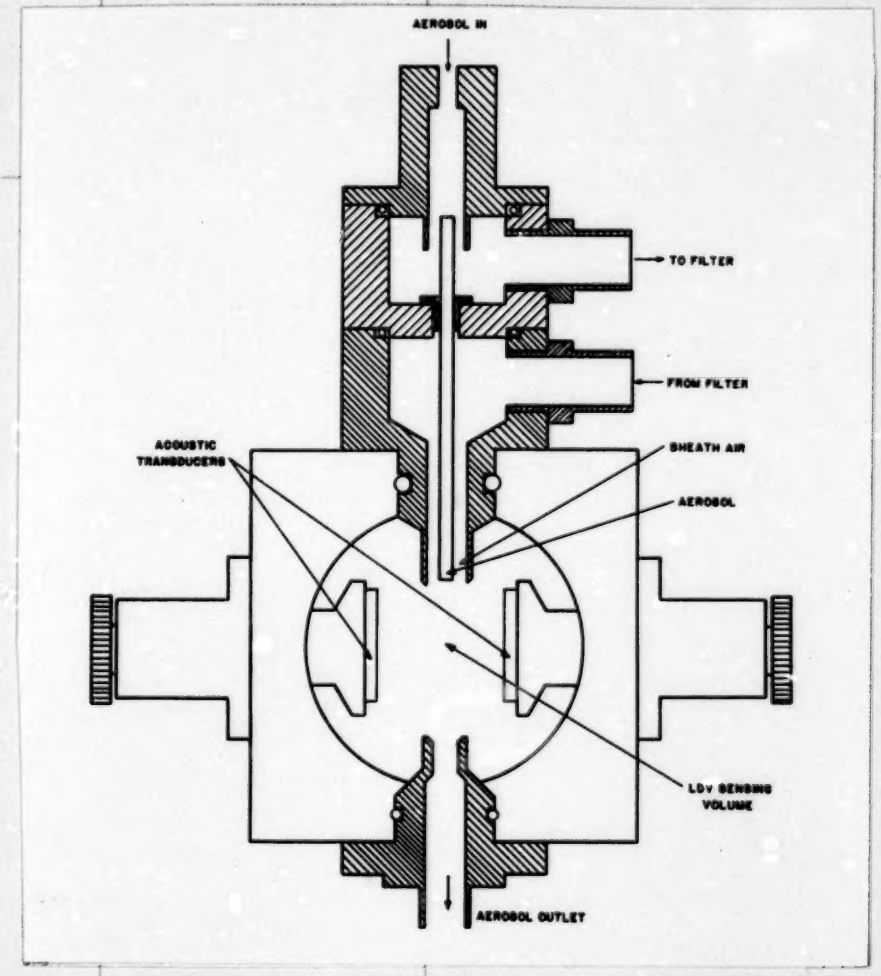

Figure 7. Schematic of the inlet to the relaxation cell.

BEGIN LAST LINE OF TEXT
3/8"
BOTTOM OF IMAGE AREA; OUTSIDE DIMENSION FOR TABLES AND ILLUSTRATIONS

EPA Form 2350-4 (4-80)
(PREVIOUSLY CIN. EPA FORM 287)
☆ U.S. GOVERNMENT PRINTING OFFICE 1980-660-639
TYPING GUIDE SHEET

BEGIN FIRST LINE OF TEXT HERE
CENTER OF PAGE
TOP OF IMAGE AREA
DROPPED HEAD; BEGIN SECTIONS HERE

A flow controller is used to establish an aerosol volumetric flow rate of 550 ml/min. The flow rate is controlled so that a particle has a residence time of 2 msec within the sensing volume. A temperature controller maintains the cell at $37^{o}C \pm 0.20$. Operating the analyzer at a known temperature is required since aerodynamic diameter depends upon the viscosity of the air (equation 12) which is a function of temperature. Human body temperature was selected as the standard so that measurements would be relevant to the inhalation of aerosols.

Acoustic transducers are located on opposite sides of the cell and are positioned symmetrically with respect to the sensing volume. The two transducers generate the standing-wave pattern; one transducer generates the acoustic drive while the other operates as a reflector and a microphone. The positions of the transducers are adjusted to locate one of the antinodes of the pattern at the LDV sensing volume. The optical axis of the LDV, the direction of flow of the aerosol sample, and the direction of the acoustic excitation are mutually orthogonal. Because the plane containing the two laser beams is perpendicular to the direction of the aerosol sample flow, the Doppler signal is insensitive to the velocity of the aerosol sample, but is sensitive to the particle velocity $V_p \sin(\omega t - \phi)$ induced by the acoustic standing wave pattern.

Because it would interfere with the aerosol flow, the microphone measuring the acoustic field cannot be located in the sensing volume. Therefore, a constant phase lag ϕ_o is introduced relative to the acoustic path length between the LDV sensing volume and the microphone. Signal and data processing circuits measure the total phase difference $\phi + \phi_o$. An externally adjustable phase-compensation circuit is used to subtract ϕ_o.

SIGNAL PROCESSING CIRCUIT

Equation (26) shows that the Doppler signal is a frequency modulated signal whose frequency deviation is proportional to the velocity of the acoustically driven particle. This FM signal can be demodulated to recover the velocity profile of the particle undergoing the acoustic excitation. Equation (26) also shows that the modulation frequency is directly proportional to the sine of half of the beam angle, θ.

Figure 8 shows a block diagram of the signal processing and data storage system of the SPART analyzer. This system consists of signal conditioning/ demodulating circuits, a phase comparator, and a microcomputer-based data processor.

The output signal from the photomultiplier tube is amplified by a two-stage, amplitude-limited RF amplifier with a center frequency of 2 MHz--the difference frequency between the Bragg cell drive frequencies--and with a bandwidth of 100 kHz. This amplified signal is demodulated by a phase-locked-loop (PLL) FM demodulator whose output signal corresponds to the

BEGIN LAST LINE OF TEXT
BOTTOM OF IMAGE AREA; OUTSIDE DIMENSION FOR TABLES AND ILLUSTRATIONS
3/8"

EPA Form 2350-4 (4-80)
(PREVIOUSLY CIN. EPA FORM 287)
☆ U.S. GOVERNMENT PRINTING OFFICE 1980-680-609
TYPING GUIDE SHEET

BEGIN FIRST LINE OF TEXT HERE
CENTER OF PAGE
TOP OF IMAGE AREA
DROPPED HEAD; BEGIN SECTIONS HERE

particle velocity in the acoustic field. The amplifier output is monitored by an RF threshold detector, which responds with a TTL logic "1" output when the RF signal level exceeds a preset value. The demodulated signal is controlled by an analog gate to ensure the output signal of the PLL is passed to the bandpass filter and the phase comparator only when the amplitude of the RF exceeds a level determined by a threshold detector. When the RF threshold signal is high, the demodulated signal is passed through an analog switch into a phase shift network which compensates for ϕ_o and any additional phase shifts introduced by the components of the signal processor, such as the amplifiers and bandpass filters. The phase shift network is adjusted during calibration of the phase-lag measurements.

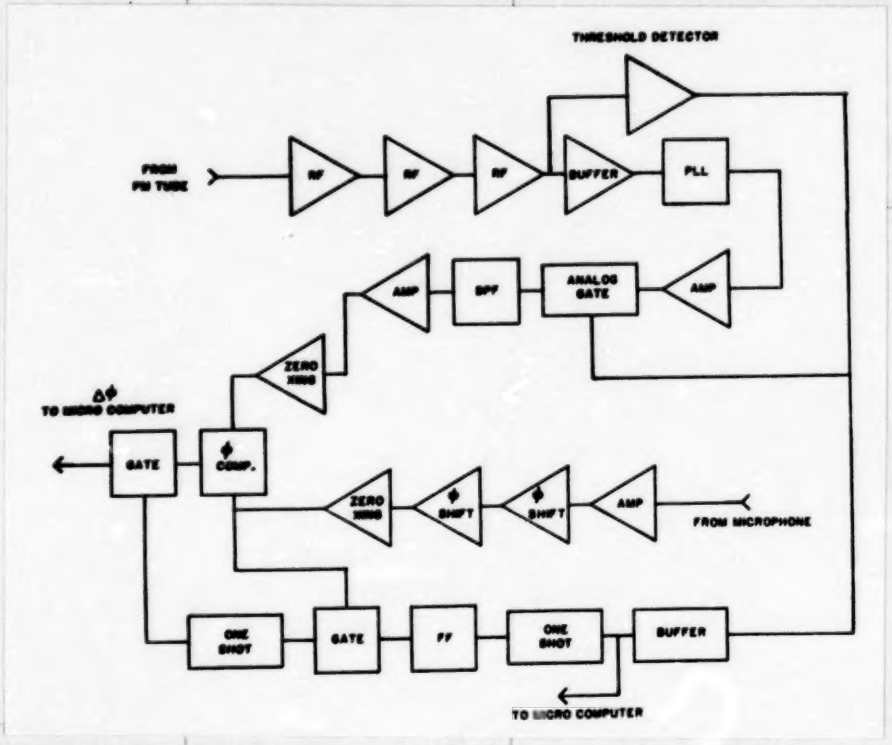

Figure 8. Block diagram of the signal processing and data storage systems of the SPART analyzer.

After passing through the externally adjustable phase shift network, the demodulated signal is filtered by a bandpass filter whose center frequency is equal to the frequency of acoustic excitation. The filtered signal is converted to a series of output pulses by a zero-crossing detector and applied to a digital phase detector circuit. The reference input to this phase detector is the output signal of the microphone, which has been amplified and then squared by a zero-crossing detector.

BEGIN LAST LINE OF TEXT
BOTTOM OF IMAGE AREA, OUTSIDE DIMENSION FOR TABLES AND ILLUSTRATIONS
3/8"

EPA Form 2350-4 (4-80)
(PREVIOUSLY CIN, EPA FORM 237)
☆ U.S. GOVERNMENT PRINTING OFFICE 1980-660-639
TYPING GUIDE SHEET

BEGIN FIRST LINE OF TEXT HERE
CENTER OF PAGE
TOP OF IMAGE AREA
DROPPED HEAD; BEGIN SECTIONS HERE

The signal-processing circuitry generates a square wave with a time interval Δt beginning at the zero crossing of the microphone signal and ending at the zero crossing of the phase-compensated demodulated LDV signal. Because there are two zero-crossings per cycle of the acoustic and demodulated signals, there are two pulses from the digital phase detector per period of acoustic wave. The time interval Δt is measured by a time interval counter that averages Δt over eight pulses from the digital phase detector. The time interval counter uses a clock oscillator whose frequency is approximately 13.8 MHz so that the number of clock pulses in Δt is proportional to Δt.

MICROCOMPUTER-BASED DATA PROCESSOR

A KIM-1 microcomputer is programmed to compute the phase delay corresponding to Δt and registers a count in a memory location, or channel, which relates to that phase shift. There are 128 such channels, each relating to a range of phase shifts. Because a given phase shift corresponds to a unique aerodynamic diameter, each channel corresponds to a known interval of aerodynamic diameter. The number of counts in a channel equals the number of particles counted which have aerodynamic diameters within the given interval. The maximum number of pulses is 128 for a maximum possible phase lag of 90°. A microcomputer sums the pulses for a given particle and increments the size channel with the corresponding number in the 128-channel data-storage system.

The number of particle counts (ΔN per channel), the size distribution $dN/d(\log d_a)$, and the volume distribution $dV/d(\log d_a)$ are computed and stored. The total sampling time, t, in seconds and the total number of counts N are recorded. The data are printed by a line printer and a Teletype generates a punched paper tape listing the number of counts in each channel in order of increasing channel number. The data from the paper tape is processed by a minicomputer to generate a graph showing the size, volume, and cumulative distributions as a function of aerodynamic diameter. The program also computes the mass median aerodynamic diameter (MMAD), count median diameter (CMD), and the geometric standard deviation (σ_g).

BEGIN LAST LINE OF TEXT
BOTTOM OF IMAGE AREA; OUTSIDE DIMENSION FOR TABLES AND ILLUSTRATIONS

EPA Form 2350-4 (4-80)
(PREVIOUSLY CIN: EPA FORM 287)
☞ U.S. GOVERNMENT PRINTING OFFICE 1980-660-825
TYPING GUIDE SHEET

BEGIN FIRST LINE OF TEXT HERE
CENTER OF PAGE
TOP OF IMAGE AREA
DROPPED HEAD; BEGIN SECTIONS HERE

SECTION 6

RESOLUTION AND RANGE

The sizing resolution of the SPART analyzer is primarily a function of two factors: (1) the relationship between $\partial\phi/\partial(d_a)$ and d_a; and (2) the electronic resolution of Δt measurements. The relationship between ϕ and d_a for a given frequency of acoustic excitation (equation 3) is nonlinear. In general, $\partial\phi/\partial(d_a)$ is high when the product $\omega\tau_p$ is close to unity. The inherent electronic resolution of Δt measurements is limited by the phase jitter noise of the phase-locked-loop demodulator and by the ± 1-pulse accuracy of counting the clock pulses. The frequency of acoustic excitation in the prototype analyzer is 27 kHz, giving an expected resolution higher than ± 0.1 μm in the range of 0.3 to 3.0 μm.

RELATIONSHIP BETWEEN $\partial\phi/\partial(d_a)$ AND d_a

SPART analyzers have their greatest sensitivity in the particle size range where ϕ changes most rapidly as a function of particle size. The size for greatest sensitivity, d_m maximizes $\partial\phi/\partial(d_a)$. The condition for a maximum is thus: $\phi''(d_a) = 0$, where the prime indicates differentiation with respect to d_a.

$$\phi'(d_a) = \omega\tau_p'/(1 + \omega^2\tau_p^2) \tag{27}$$

and

$$\phi''(d_a) = [(1 + \omega^2\tau_p^2)\omega\tau_p'' - 2\omega^3\tau_p(\tau_p')^2]/(1 + \omega^2\tau_p^2)^2 \tag{28}$$

Therefore, the equation

$$(1 + \omega^2\tau_p^2)(\omega\tau_p'') = 2(\omega\tau_p)(\omega\tau_p')^2 \tag{29}$$

can be solved for determining d_m.

For particles large enough so that $C_c \approx 1$, equation (29) can be simplified, with the result that

$$\omega\tau_p = 1/3^{1/2} \tag{30}$$

or

BEGIN LAST LINE OF TEXT
BOTTOM OF IMAGE AREA; OUTSIDE DIMENSION FOR TABLES AND ILLUSTRATIONS
3/8"

EPA Form 2350-4 (4-80)
(PREVIOUSLY CIN: EPA FORM 287)
U.S. GOVERNMENT PRINTING OFFICE 1980-660-639
TYPING GUIDE SHEET

BEGIN FIRST LINE OF TEXT HERE
CENTER OF PAGE
TOP OF IMAGE AREA

$$f = (3)(3)^{1/2}\eta/\pi\rho_o d_a^2 \qquad (31)$$

Thus,

$$\phi = \tan^{-1}(1/3^{1/2}) = 30^o. \qquad (32)$$

DROPPED HEAD; BEGIN SECTIONS HERE

Under this condition, the value of μ in equation (21) is 0.866. Equation (32) gives the phase angle for maximum resolution. The channel number for greatest resolution is given approximately by

$$n_c = n_m/3 \qquad (33)$$

where n_m is the channel number (128) corresponding to the maximum phase angle (90^o). Figure 9 shows the acoustic excitation frequency for optimum size resolution as a function of d_a. Figure 9 indicates that the acoustic frequency must be increased, close to 100 kHz, for an optimum resolution for d_a in the range of 0.1 μm. However, in practice a SPART analyzer can be operated at an excitation frequency well below 100 kHz without any significant loss of resolution provided it is possible to measure Δt for a small value of ϕ.

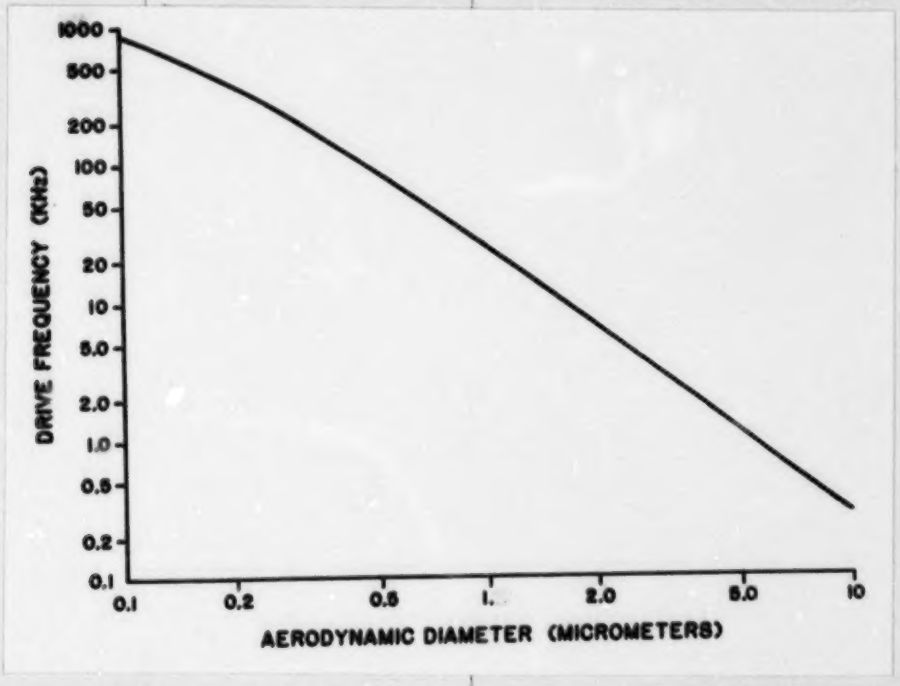

Figure 9. Acoustic excitation frequency for optimum size resolution as a function of d_a.

BEGIN LAST LINE OF TEXT
BOTTOM OF IMAGE AREA; OUTSIDE DIMENSION FOR TABLES AND ILLUSTRATIONS
3/8"

EPA Form 2350-4 (4-80)
(PREVIOUSLY CIN. EPA FORM 287)
☆ U.S. GOVERNMENT PRINTING OFFICE 1980-680-639
TYPING GUIDE SHEET

BEGIN FIRST LINE OF TEXT HERE
CENTER OF PAGE
TOP OF IMAGE AREA
DROPPED HEAD; BEGIN SECTIONS HERE

From equation (11),

$$\phi = \tan^{-1}(\omega\tau_p) .$$

When ϕ is small,

$$\tan(\phi) \simeq \phi . \qquad (34)$$

Thus,

$$\tau_p \simeq \phi/\omega . \qquad (35)$$

Since

$$\phi = 2\pi f\Delta t = \omega\Delta t, \qquad (36)$$

$$\tau_p = \omega\Delta t/\omega = \Delta t, \text{ for } \phi < 5^{\circ} . \qquad (37)$$

The right side of this equation is independent of the frequency of excitation and shows that Δt is an approximate measure of τ_p. Thus, the resolution at the lower limit of aerodynamic diameter is determined by the resolution of Δt measurements and the signal-to-noise ratio of the phase lag measuring circuits.

RESOLUTION OF Δt MEASUREMENT

The phase lag ϕ between the motion of the particle and the driving force is obtained by measuring the time lag Δt between the drive signal and the LDV signal. The relation between ϕ and Δt (equation 36) is $\phi = \omega\Delta t$.

The signal processing circuit measures Δt by digitally counting the periods of an oscillator whose frequency, f_s, is much greater than the drive frequency f. The result of this counting is the channel number n_c of the particle being measured. Thus,

$$n_c = f_s\Delta t \qquad (38)$$

and from equations (36) and (11), the above equation can be written as

$$n_c = (f_s/\omega)\tan^{-1}(\omega\tau_p) . \qquad (39)$$

Since the greatest value of the inverse tangent function is $\pi/2$, there is a maximum channel number, n_m, given by

$$n_m = (f_s/2\pi f)(\pi/2) = f_s/4f \qquad (40)$$

where, since n_m is an integer, n_m should be equal to the least integer greater than or equal to the right side of equation (40).

BEGIN LAST LINE OF TEXT
BOTTOM OF IMAGE AREA; OUTSIDE DIMENSION FOR TABLES AND ILLUSTRATIONS

EPA Form 2350-4 (4-80)
(PREVIOUSLY CIN. EPA FORM 287)
© U.S. GOVERNMENT PRINTING OFFICE 1980-660-639
TYPING GUIDE SHEET

BEGIN FIRST LINE OF TEXT HERE
CENTER OF PAGE
TOP OF IMAGE AREA

Writing n_c as a function of d_a,

$$n_c = (f_s/2\pi f)\tan^{-1}(2\pi F \rho_o d_a^2 C_{ca}/18\eta) . \qquad (41)$$

DROPPED HEAD; BEGIN SECTIONS HERE

Table 1 is a listing of values of d_a corresponding to the integer values of n_c for f = 27.0 kHz and f_s = 13.824 MHz -- the frequencies used by one of the breadboard SPART analyzers. In Table 2, the lower edges are tabulated (the lower edge of channel 2 equals the upper edge of channel 1) along with the geometric mean diameter - the square root of the product of the upper and lower edges.

The frequency of acoustic drive varied from 23 to 27 kHz depending upon the ultrasonic transducers used in the breadboard analyzers. A small variation of f does not change the channel numbers significantly as is expected from the theory. For example, channel #45 corresponds to 1.00 μm at f = 27.0 kHz (Table 1) and to 1.06 μm at f = 24.25 kHz (Table 2). Each of the breadboard analyzers was constructed with a pair of acoustic transducers that had nearly identical resonance frequency characteristics. To change the effective size range of the SPART analyzer, the frequency of the acoustic drive signal can be adjusted according to the plots shown in Figure 2. When the value of f is lowered significantly, the range of operation changes significantly as shown in Table 3.

Tables 2 and 3 show that, in principle, the SPART analyzer will resolve exceedingly narrow size distribution if optimum values of f are chosen and the ratio of f_s/f is high. However, in practice, the resolution will be limited by signal-to-noise ratio (SNR) of the phase detection. The size resolution was experimentally determined by measuring the geometric standard deviation (σ_g) of the indicated size distribution of monodisperse PLS aerosol of known size.

SIZE RANGE

The effective size range depends upon the SNR of the LDV signal as a function of d_a which in turn depends upon the laser power, the geometry of the receiving optics, and the quantum efficiency of the detector. The scattered light received from each particle by the detector must generate a Doppler signal with an SNR above a threshold value so the signal-processing electronics can demodulate the FM signal burst. A particle is not detected when its signal does not have an SNR above the threshold limit. This threshold limit is often set by the Rayleigh scattering from the air molecules inside the sensing volume and by the electronic noise. Once the signal meets the SNR requirement, the size-detection process is independent of the magnitude of the intensity of scattered light incident on the detector.

BEGIN LAST LINE OF TEXT
BOTTOM OF IMAGE AREA; OUTSIDE DIMENSION FOR TABLES AND ILLUSTRATIONS
3/8"

EPA Form 2350-4 (4-80)
(PREVIOUSLY CIN. EPA FORM 287)
☆ U.S. GOVERNMENT PRINTING OFFICE: 1980-660-639
TYPING GUIDE SHEET

BEGIN FIRST LINE OF TEXT HERE
CENTER OF PAGE
TOP OF IMAGE AREA
DROPPED HEAD; BEGIN SECTIONS HERE

TABLE 1

C_{ca}, τ_p, ϕ, Δt, and n_c as a function of d_a for

f = 27.0 kHz, f_s = 13.824 MHz

d_a μm	C_{ca}	τ_p μs	ϕ Degrees	Δt μs	n_c (Channel Number)
0.08	3.38	0.067	0.65	0.069	1
0.09	3.09	0.077	0.75	0.077	2
0.10	2.87	0.084	0.86	0.088	2
0.20	1.87	0.23	2.24	0.23	4
0.30	1.56	0.43	4.21	0.43	6
0.40	1.41	0.70	6.76	0.79	10
0.50	1.33	1.03	9.88	1.02	15
0.60	1.27	1.42	13.50	1.39	20
0.70	1.23	1.87	17.58	1.81	25
0.80	1.21	2.38	21.99	2.26	32
0.90	1.18	2.96	26.63	2.74	38
1.00	1.16	3.59	31.36	3.23	45
2.00	1.08	13.36	66.19	6.81	95
3.00	1.05	29.30	78.62	8.09	112
4.00	1.04	51.41	83.46	8.59	119
5.00	1.03	79.69	85.77	8.82	122
6.00	1.02	114.20	87.04	8.96	124
7.00	1.02	154.78	87.82	9.03	125
8.00	1.02	201.58	88.33	9.09	126
9.00	1.01	254.56	88.67	9.12	127
10.00	1.01	313.70	88.92	9.15	127
20.00	1.01	1244.70	89.73	9.23	128

6 1/2"
3 1/8"
BEGIN LAST LINE OF TEXT
3/8"
BOTTOM OF IMAGE AREA; OUTSIDE DIMENSION FOR TABLES AND ILLUSTRATIONS

EPA Form 2350-4 (4-80)
(PREVIOUSLY CIN. EPA FORM 287)
☆ U.S. GOVERNMENT PRINTING OFFICE 1980-660-639
TYPING GUIDE SHEET

BEGIN FIRST LINE OF TEXT HERE

CENTER OF PAGE

TOP OF IMAGE AREA

DROPPED HEAD: BEGIN SECTIONS HERE

TABLE 2

Channel Numbers vs Aerodynamic Diameters

Sampling Frequency = 12.416 MHz Driving Frequency = 24.250 kHz

Channel Number n_c	Median d_a in µm	Channel Number n_c	Median d_a in µm	Channel Number n_c	Median d_a in µm
1	0.00	44	1.04	87	1.87
2	0.12	45	1.06	88	1.90
3	0.18	46	1.07	89	1.93
4	0.23	47	1.09	90	1.96
5	0.26	48	1.10	91	1.98
6	0.30	49	1.12	92	2.02
7	0.34	50	1.14	93	2.06
8	0.37	51	1.15	94	2.09
9	0.40	52	1.17	95	2.13
10	0.42	53	1.18	96	2.17
11	0.45	54	1.20	97	2.21
12	0.47	55	1.22	98	2.25
13	0.50	56	1.23	99	2.29
14	0.51	57	1.25	100	2.33
15	0.54	58	1.27	101	2.38
16	0.56	59	1.29	102	2.43
17	0.58	60	1.30	103	2.48
18	0.60	61	1.32	104	2.54
19	0.62	62	1.33	105	2.60
20	0.64	63	1.35	106	2.66
21	0.66	64	1.37	107	2.72
22	0.68	65	1.39	108	2.80
23	0.70	66	1.41	109	2.87
24	0.72	67	1.42	110	2.95
25	0.73	68	1.44	111	3.04
26	0.75	69	1.46	112	3.14
27	0.77	70	1.48	113	3.24
28	0.78	71	1.50	114	3.36
29	0.80	72	1.52	115	3.49
30	0.82	73	1.54	116	3.63
31	0.84	74	1.56	117	3.79
32	0.85	75	1.58	118	3.97
33	0.87	76	1.60	119	4.18
34	0.88	77	1.62	120	4.43
35	0.90	78	1.65	121	4.72
36	0.92	79	1.67	122	5.08
37	0.93	80	1.69	123	5.54
38	0.95	81	1.72	124	6.14
39	0.96	82	1.74	125	6.99
40	0.98	83	1.76	126	8.32
41	0.99	84	1.79	127	10.98
42	1.01	85	1.82	128	99.99
43	1.03	86	1.84		

9-1/2"

9-1/8"

BEGIN LAST LINE OF TEXT

3/8"

BOTTOM OF IMAGE AREA, OUTSIDE DIMENSION FOR TABLES AND ILLUSTRATIONS

EPA Form 2350-4 (4-80)

(PREVIOUSLY CIN. EPA FORM 287)

☆ U.S. GUVERNMENT PRINTING OFFICE 1980-660-638

TYPING GUIDE SHEET

BEGIN FIRST LINE OF TEXT HERE
CENTER OF PAGE
TOP OF IMAGE AREA
DROPPED HEAD; BEGIN SECTIONS HERE

TABLE 3

Channel Numbers vs Aerodynamic Diameters

Sampling Frequency = 12.416 MHz Driving Frequency = 2.425 kHz

Channel Number n_c	Median d_a in µm	Channel Number n_c	Median d_a in µm	Channel Number n_c	Median d_a in µm
1	0.00	44	3.46	87	6.08
2	0.53	45	3.51	88	6.18
3	0.72	46	3.56	89	6.27
4	0.87	47	3.61	90	6.37
5	1.00	48	3.66	91	7.47
6	1.12	49	3.71	92	6.57
7	1.22	50	3.76	93	6.67
8	1.32	51	3.81	94	6.78
9	1.41	52	3.86	95	6.90
10	1.50	53	3.91	96	7.02
11	1.58	54	3.97	97	7.14
12	1.66	55	4.02	98	7.27
13	1.73	56	4.07	99	7.41
14	1.80	57	4.12	100	7.55
15	1.87	58	4.17	101	7.70
16	1.94	59	4.23	102	7.86
17	2.01	60	4.28	103	8.02
18	2.07	61	4.33	104	8.19
19	2.14	62	4.39	105	8.38
20	2.20	63	4.44	106	8.58
21	2.26	64	4.50	107	8.78
22	2.31	65	4.56	108	9.01
23	2.37	66	4.61	109	9.25
24	2.43	67	4.67	110	9.50
25	2.49	68	4.73	111	9.78
26	2.54	69	4.79	112	10.09
27	2.60	70	4.85	113	10.42
28	2.65	71	4.91	114	10.78
29	2.70	72	4.98	115	11.18
30	2.76	73	5.04	116	11.63
31	2.81	74	5.10	117	12.14
32	2.86	75	5.17	118	12.71
33	2.91	76	5.24	119	13.37
34	2.96	77	5.31	120	14.15
35	3.01	78	5.38	121	15.07
36	3.06	79	5.45	122	16.20
37	3.11	80	5.52	123	17.63
38	3.16	81	5.60	124	19.50
39	3.21	82	5.67	125	22.15
40	3.26	83	5.75	126	26.29
41	3.31	84	5.83	127	34.39
42	3.36	85	5.91	128	91.27
43	3.41	86	5.99	129	99.99

6 1/2"
9-1/8"
BEGIN LAST LINE OF TEXT
3/8"
BOTTOM OF IMAGE AREA, OUTSIDE DIMENSION FOR TABLES AND ILLUSTRATIONS

EPA Form 2350-4 (4-80)
(PREVIOUSLY CIN, EPA FORM 287)
☆ U.S. GOVERNMENT PRINTING OFFICE 1980-660-639
TYPING GUIDE SHEET

BEGIN FIRST LINE OF TEXT HERE
CENTER OF PAGE
TOP OF IMAGE AREA
DROPPED HEAD; BEGIN SECTIONS HERE

SECTION 7

COUNT RATE AND COINCIDENCE LOSS

EFFECTIVE SAMPLING RATE

The intensity of the light scattered by a particle transiting the sensing volume depends upon the Gaussian intensity distribution of the laser beams at the beam intersection and the optical properties of the particle. If the particle velocity in the direction of the aerosol sample flow is U_s and if the effective cross-sectional area of the sensing volume in this direction is A_s, then

$$dN/dt = N_o A_s U_s, \qquad (42)$$

where dN/dt is the count per second registered by the SPART analyzer and N_o is the number concentration of the aerosol in particles per unit volume. The SPART analyzer can count particles at a maximum rate of 200 particles per second. However, a high count rate will result in a large coincidence error and a low count rate will have poor statistical accuracy. The optimal count rate generally is from 1 to 40 counts per second.

The effective sampling flow rate $Q(d_a)$ of the aerosol sample through the sensing volume in cubic centimeters per second can be defined as

$$Q(d_a) = A_s U_s. \qquad (43)$$

The value of $Q(d_a)$ is a function of d_a because A_s, for a given optical geometry, varies with d_a. In other words, the amplitude of the Doppler signal generated by particles transiting a given trajectory through the sensing volume depends upon the particle size. For example, a small particle transiting the peripheral region of the sensing volume may not generate a signal of sufficient magnitude for the analyzer to detect the particle; however, a large particle traveling through the same region may generate a detectable signal.

A nominal value of A_s can be estimated from the optical beam geometry of the transmission and the receiving optics of the LDV. Because $Q(d_a)$ is proportional to A_s, it is desirable to make A_s as large as possible so that the counting rate will be large. Assuming that the laser beams are cylindrical in the vicinity of the sensing volume (see Figure 6), the following formulas apply assuming diffraction limited optics is in the arrangement shown in Figure 6.

BEGIN LAST LINE OF TEXT
BOTTOM OF IMAGE AREA; OUTSIDE DIMENSION FOR TABLES AND ILLUSTRATIONS
3/8"

EPA Form 2350-4 (4-80)
(PREVIOUSLY CIN. EPA FORM 287)
☆ U.S. GOVERNMENT PRINTING OFFICE 1980-660-639
TYPING GUIDE SHEET

BEGIN FIRST LINE OF TEXT HERE
CENTER OF PAGE
TOP OF IMAGE AREA

$$A_s = d_f^2/\sin(\theta), \qquad (44)$$

where d_f is the $1/e^2$ Gaussian beam diameter at the focal point of the lens (diffraction limit) and θ is the angle between the beams.

DROPPED HEAD: BEGIN SECTIONS HERE

$$d_f = 3.18\lambda f/D_{(1/e^2)} \qquad (45)$$

where λ is the wavelength of the laser radiation, f is the focal length of the lens, and $D_{(1/e^2)}$ is the $1/e^2$ Gaussian beam diameter of the unfocussed laser beams and since

$$f = S/[2\tan(\theta/2)] \qquad (46)$$

where S is the distance between the beam centers when the beams enter the lens. It follows that

$$A_s = 2.53\lambda^2 S^2/[D_{(1/e)}{}^2 \sin(\theta)\tan^2(\theta/2)]. \qquad (47)$$

6-1/2"

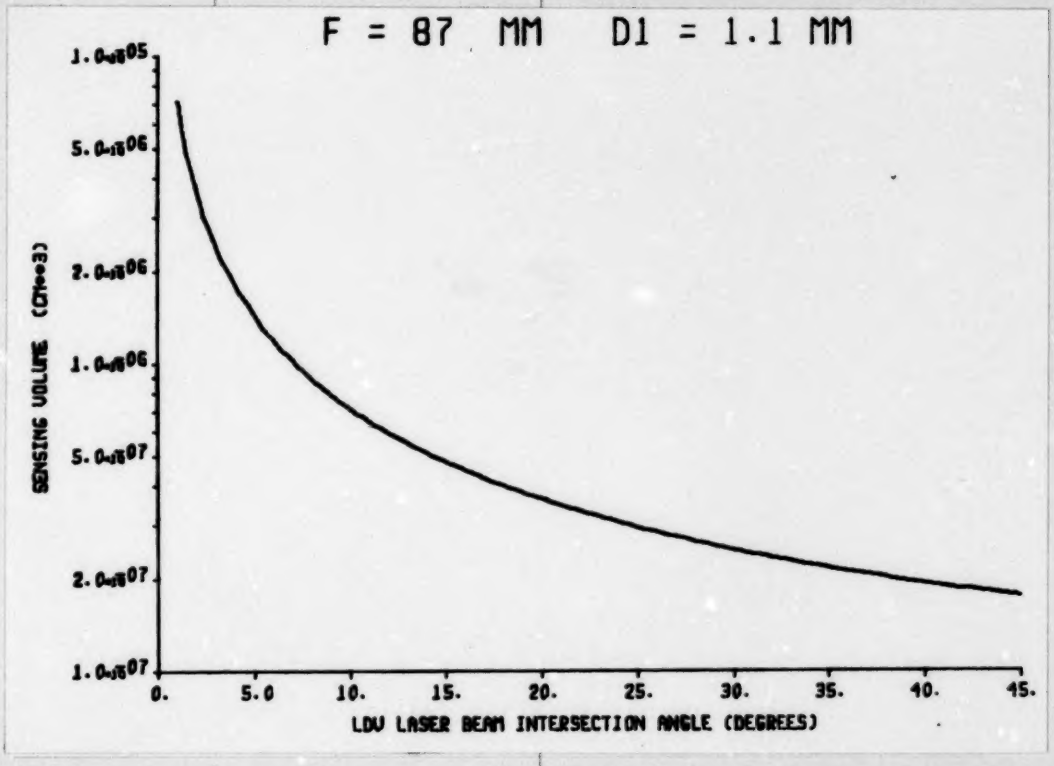

Figure 10. Calculated value of the LDV probe volume v_s plotted as a function of the laser beam intersection angle θ; for S = 5 cm, f = 8.7 cm, $D(1/e^2)$ = 1.1 mm and λ = 488 nm.

BEGIN LAST LINE OF TEXT
BOTTOM OF IMAGE AREA OUTSIDE DIMENSION FOR TABLES AND ILLUSTRATIONS
3/8"

EPA Form 2350-4 (4-80)
(PREVIOUSLY CIN, EPA FORM 247)
☆ U.S. GOVERNMENT PRINTING OFFICE 1980-660-539
TYPING GUIDE SHEET

BEGIN FIRST LINE OF TEXT HERE
CENTER OF PAGE
TOP OF IMAGE AREA

Figure 10 is a plot of calculated values of the LDV probe volume v_s (equation 23) versus θ for a fixed value of S (S = 5 cm). Because of the variation of d_f with f, the laser power density in the sensing volume will be proportional to f^{-2}. This sets an upper limit on f. When this limit is determined, A_s can be increased further by decreasing S.

DROPPED HEAD; BEGIN SECTIONS HERE

A higher value of $Q(d_a)$ is desired in order to permit dN/dt to be reasonably high even when N_o is low. However, an increase in A_s also increases the LDV sensing volume. A large sensing volume causes a larger coincidence loss[4] when the particulate concentration is high. Further, if θ is reduced for increasing A_s, the frequency deviation of the Doppler signal (equation 26), being proportional to $\sin(\theta/2)$ also decreases, resulting in a smaller amplitude of the demodulated LDV signal output. A compromise is therefore necessary to adjust A_s to obtain the optimal value of $Q(d_a)$ for measuring particulate concentration in a given range.

COINCIDENCE ERROR

6-1/2"

The sensing volume (V_s) of this LDV-based instrument is approximately 10^{-5} cc. Such a small sensing volume allows measurement of the size distribution of aerosol particulates with a relatively high number concentration without significant coincidence errors. The concidence C can be expressed as follows:

$$C = 1 - \exp(-N_o V_s), \tag{48}$$

where N_o is the number of particles per cubic centimeter and V_s is the sensing volume. The above expression can be written in terms of the transit time (τ_R) of the particles crossing the LDV sensing volume:

$$C = 1 - \exp(-N_t \tau_R), \tag{49}$$

where N_t is the number of particle bursts per unit time registered by the SPART analyzer. Writing N_t in the form

$$N_t = -\ln(1 - C)/\tau_R \tag{50}$$

shows that for τ_R = 500 μs, the coincidence error would be 4.8 percent for a particle count rate of 100 particles/sec.

Errors caused by coincidence in the SPART analyzer must be distinguished from the coincidence error in optical particle counters. Experimental studies performed on the SPART analyzer on coincidence losses have shown that while counting monodisperse 0.8 μm polystyrene latex spheres (PLS), the geometric standard deviation of the measured CMD increased from 1.07 to 1.09 when the particle count per second was increased from 40 particles/sec to 400 particles/sec. Similar measurements were performed with polydisperse dioctylsebacate (DOS) aerosol and no significant difference in the size

BEGIN LAST LINE OF TEXT
BOTTOM OF IMAGE AREA; OUTSIDE DIMENSION FOR TABLES AND ILLUSTRATIONS
3/8"

EPA Form 2350-4 (4-80)
(PREVIOUSLY CIN. EPA FORM 287)
☆ U.S. GOVERNMENT PRINTING OFFICE 1980-660-639
TYPING GUIDE SHEET

BEGIN FIRST LINE OF TEXT HERE
CENTER OF PAGE
TOP OF IMAGE AREA
DROPPED HEAD; BEGIN SECTIONS HERE

distribution was observed when the particle count per second was increased from 14 particles/sec to 362 particles/sec. These data shown in Table 4 and 5 indicate the SPART analyzer can count up to 400 particles/sec without any significant measurement error in the size distribution. When an optical particle counter (Climet 208) was tested for similar coincidence loss, the standard deviation of the measured CMD increased from 2.3 to 16.4. The most plausible explanation for the immunity of the SPART analyzer in particle sizing from coincidence error is that the measurement is independent of the intensity of the scattered light.

In the SPART analyzer, the measurement of size distribution and transit time τ_R, as well as that of the particle count rate N_t, can be performed in real time. The particulate concentration can thus be corrected if desired, with the measured value of C as shown in equation (50), thereby making it possible to obtain an unbiased size distribution while counting at a rate of 100 particles/sec.

In the prototype SPART III analyzer, the calculated sensing volume is approximately 1.3×10^{-6} cm^3, A_s is approximately 2.8×10^{-4} cm^2, and U_s is approximately 15 cm/sec. From equation (43), the calculated value of $Q(d_a)$ is approximately 4.0×10^{-3} cm^3/sec. The coincidence loss calculated from the value of the sensing volume is approximately one percent for $N_o \simeq 5 \times 10^3$ particles per cubic centimeter. When $N_o > 10^5$ particles per cubic centimeter, the aerosol can be diluted by a known amount. Thus, the low coincidence error in the SPART analyzer makes it suitable for measuring the size distribution of submicron particulates with a relatively high concentration. The counting statistics limit the lowest particulate concentration that the analyzer can measure.[9] The analyzer is also limited by poor counting statistics at $N_o < 10$ particles per cubic centimeter. When $N_o < 10$ particles per cubic centimeter (e.g., atmospheric concentration of particulates with d_a greater than 3 μm), the required sampling time t becomes large, in the order of hours. It is possible, however, to vary $Q(d_a)$ over a wide range by modifying the LDV optics for measuring particulate concentrations in the size range 0.1 to 10.0 μm.

BEGIN LAST LINE OF TEXT
BOTTOM OF IMAGE AREA; OUTSIDE DIMENSION FOR TABLES AND ILLUSTRATIONS
3/8"

EPA Form 2350-4 (4-80)
(PREVIOUSLY CIN. EPA FORM 287)
☆ U.S. GOVERNMENT PRINTING OFFICE 1980-660-639
TYPING GUIDE SHEET

BEGIN FIRST LINE OF TEXT HERE
CENTER OF PAGE
TOP OF IMAGE AREA
DROPPED HEAD; BEGIN SECTIONS HERE
6 1/2"
9-1/8"
BEGIN LAST LINE OF TEXT
3/8"
BOTTOM OF IMAGE AREA; OUTSIDE DIMENSION FOR TABLES AND ILLUSTRATIONS
PAGE NUMBER
EPA Form 2350-4 (4-80)
(PREVIOUSLY CIN. EPA FORM 287)
☆ U.S. GOVERNMENT PRINTING OFFICE 1980-660-639
TYPING GUIDE SHEET

TABLE 4

Effect of Coincidence Loss on the Size Distribution of Monodisperse 0.804 μm Polystyrene Latex Spheres as Measured by the SPART Analyzer

Counts/sec N_t	Coincidence Loss	CMD (μm)	MMAD (μm)	σ_g
13	0.003	0.79	0.79	1.07
38	0.008	0.80	0.80	1.07
412	0.095	0.79	0.79	1.09

TABLE 5

Effect of Coincidence Loss on the Measured Size Distribution of Polydisperse DOS Aerosol as Measured by the SPART Analyzer

Counts/sec N_t	Coincidence Loss C	Measured CMD μm	Measured MMAD μm	Measured σ_g
13.6	0.003	0.87	1.55	1.53
14.2	0.003	0.87	1.55	1.53
184.0	0.040	0.86	1.52	1.53
185.0	0.050	0.86	1.49	1.52
354.0	0.079	0.88	1.76	1.52
362.0	0.081	0.87	1.62	1.51

BEGIN FIRST LINE OF TEXT HERE
CENTER OF PAGE
TOP OF IMAGE AREA
DROPPED HEAD; BEGIN SECTIONS HERE

SECTION 8

TEST RESULTS

CALIBRATION: AERODYNAMIC SIZE

Size calibration of the instrument was accomplished by using a monodisperse aerosol containing polystyrene latex spheres (PLS). The instrument does not require size calibration if the measurement of $\phi + \phi_o$ is performed accurately and ϕ_o is subtracted. In practice accurate measurement of ϕ_o is difficult; however, calibration of the analyzer with a monodisperse aerosol of known aerodynamic diameter is relatively simple.

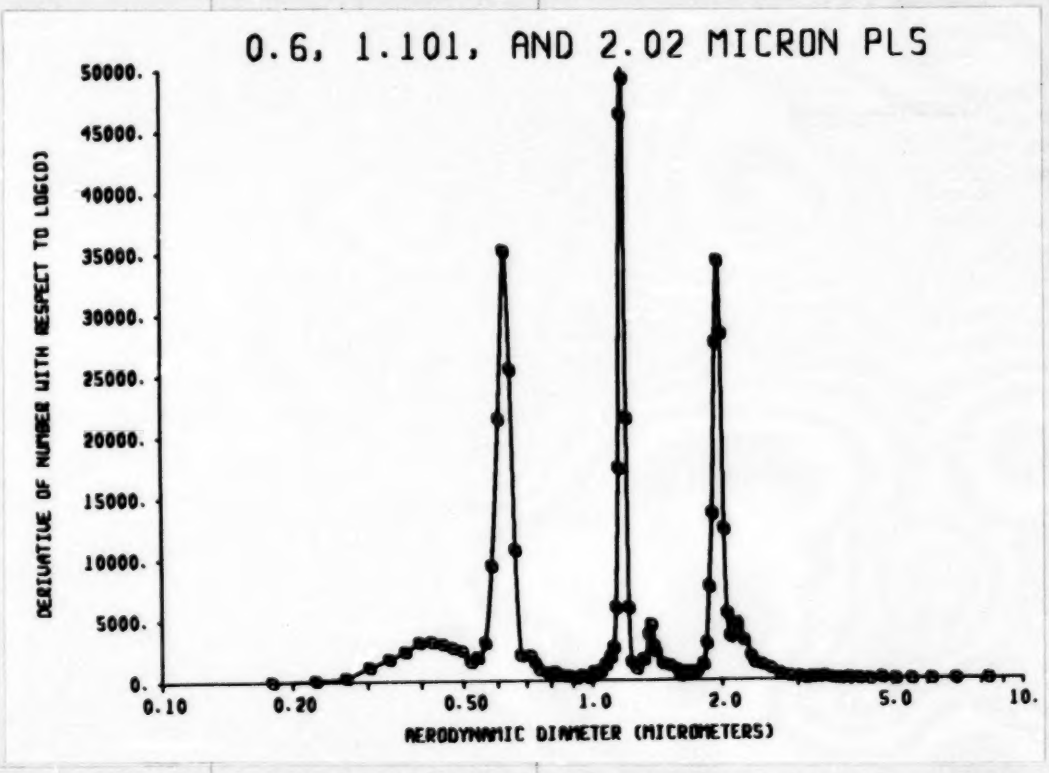

Figure 11. Number distributions of aerosol particles containing a mixture of three sizes of PLS as measured by the SPART analyzer after calibration with 0.804 μm PLS aerosol.

BEGIN LAST LINE OF TEXT
3/8"
BOTTOM OF IMAGE AREA OUTSIDE DIMENSION FOR TABLE AND ILLUSTRATIONS

EPA Form 2350-4 (4-80)
(PREVIOUSLY O'N. EPA FORM 287)
☆ U.S. GOVERNMENT PRINTING OFFICE 1980-660-639
TYPING GUIDE SHEET

Because PLS are spherical with a density of 1.05 gm/cm^3, their geometric diameter is close to the aerodynamic diameter. The analyzer was calibrated using 0.804 μm diameter PLS aerosol. That is, the peak of the number distribution of the 0.804 μm PLS aerosol was set to the channel number calculated from the expected value of ϕ by adjusting an offset to subtract the appropriate value of ϕ_o. Once this calibration is performed, the size spectra experimentally obtained from particles of other known sizes should agree with the expected distributions within experimental error. Figure 11 shows the number distributions of PLS aerosol mixture with d_a = 0.600, 1.101 and 2.02 μm that were analyzed separately. The monodisperse aerosols were generated by using a Collison atomizer for PLS aerosols. A Berglund-Liu[10] aerosol generator was used for generative olive oil aerosols with droplet sizes greater than 2.0 μm. The experimental data have been reported earlier.[11]

CALIBRATION: AEROSOL PARTICULATE CONCENTRATION

The measurement of aerosol concentration as a function of aerodynamic diameter was performed by using the Berglund-Liu generator and a Climet optical particle counter.[12,13] The Berglund-Liu generator produces a monodisperse aerosol of known concentration; thus, the measured value of the count rate registered by the SPART analyzer can be used to determine $Q(d_a)$ for the particulate size used. The Berglund-Liu generator cannot be used conveniently in the submicron range. For the size range 0.3-1 μm, the experimental value of $Q(d_a)$ was obtained by using PLS aerosols generated by the Collison atomizer, and the concentration of the aerosol was determined by using the Climet counter.

Figure 12 shows the experimentally obtained relationship between $Q(d_a)$ and d_a in the size range 0.3-6.0 μm. The experimental data indicate that the SPART analyzer has a lower size limit of 0.3 μm. Because of the large variation of $Q(d_a)$ below this size limit, the number of counts registered below this lower limit were ignored in calculating the particulate concentrations. Ideally, it is desirable to have a constant value of $Q(d_a)$ within a given size range in d_a. The variation of $Q(d_a)$ vs d_a in the range 0.3 to 6.0 μm was probably a result of the Mie scattering intensity variations of test aerosol particles used. The exact values of $Q(d_a)$ given in Figure 12 can be used only for the same particles as used for calibrating the analyzer. The average value of $Q(d_a)$ for different aerosol particles in the size range 0.3 to 6.0 μm was found to be 0.01 cm^3/sec. This is approximately 2.5 times larger than the calculated value discussed in the previous section. The difference is probably due to the LDV sensing volume being larger than was estimated assuming diffraction limited optics. Apparently, it will be necessary to develop a scheme for automatic correction for this variation of $Q(d_a)$ in the analyzer for measuring particulate concentration of unknown aerosol samples.

BEGIN FIRST LINE OF TEXT HERE
CENTER OF PAGE
TOP OF IMAGE AREA
DROPPED HEAD: BEGIN SECTIONS HERE
6-1/2"
BEGIN LAST LINE OF TEXT
3/8"
BOTTOM OF IMAGE AREA; OUTSIDE DIMENSION FOR TABLES AND ILLUSTRATIONS
PAGE NUMBER
EPA Form 2350-4 (4-80)
(PREVIOUSLY CIN: EPA FORM 2871)
☆ U.S. GOVERNMENT PRINTING OFFICE 1980 680-629
TYPING GUIDE SHEET

BEGIN FIRST LINE OF TEXT HERE
CENTER OF PAGE
TOP OF IMAGE AREA
DROPPED HEAD; BEGIN SECTIONS HERE

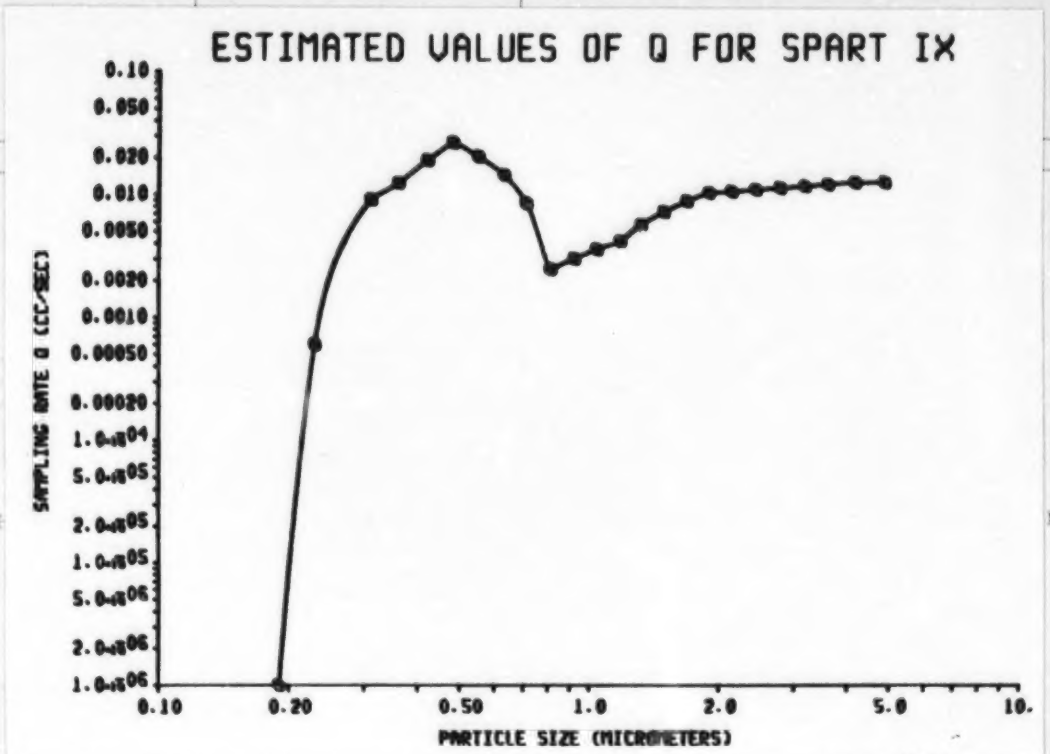

Figure 12. Experimentally observed values of the effective sampling rate $Q(d_a)$ plotted as a function of d_a.

A method of correction based on the simultaneous measurement of the transit time of the particles through the LDV sensing volume is currently under development. Meanwhile, a constant value 0.010 for $Q(d_a)$ is assumed in the size range 0.3 to 6.0 μm for plotting size distributions (for example, Figures 13 and 14).

MEASUREMENT OF AEROSOL SIZE DISTRIBUTION

The SPART was used to measure the size distributions of stable and unstable test aerosols. Results of some of the test runs are presented here to show the dynamic range and typical applications of the analyzer. The SPART is now being applied to studies of atmospheric aerosol (Figure 13) and to the characterization of medical aerosols.[14,15]

BEGIN LAST LINE OF TEXT
3/8"
BOTTOM OF IMAGE AREA; OUTSIDE DIMENSION FOR TABLES AND ILLUSTRATIONS

EPA Form 2350-4 (4-80)
(PREVIOUSLY CIN. EPA FORM 287)
☆ U.S. GOVERNMENT PRINTING OFFICE 1980-660-639
TYPING GUIDE SHEET

BEGIN FIRST LINE OF TEXT HERE
CENTER OF PAGE
TOP OF IMAGE AREA
DROPPED HEAD; BEGIN SECTIONS HERE

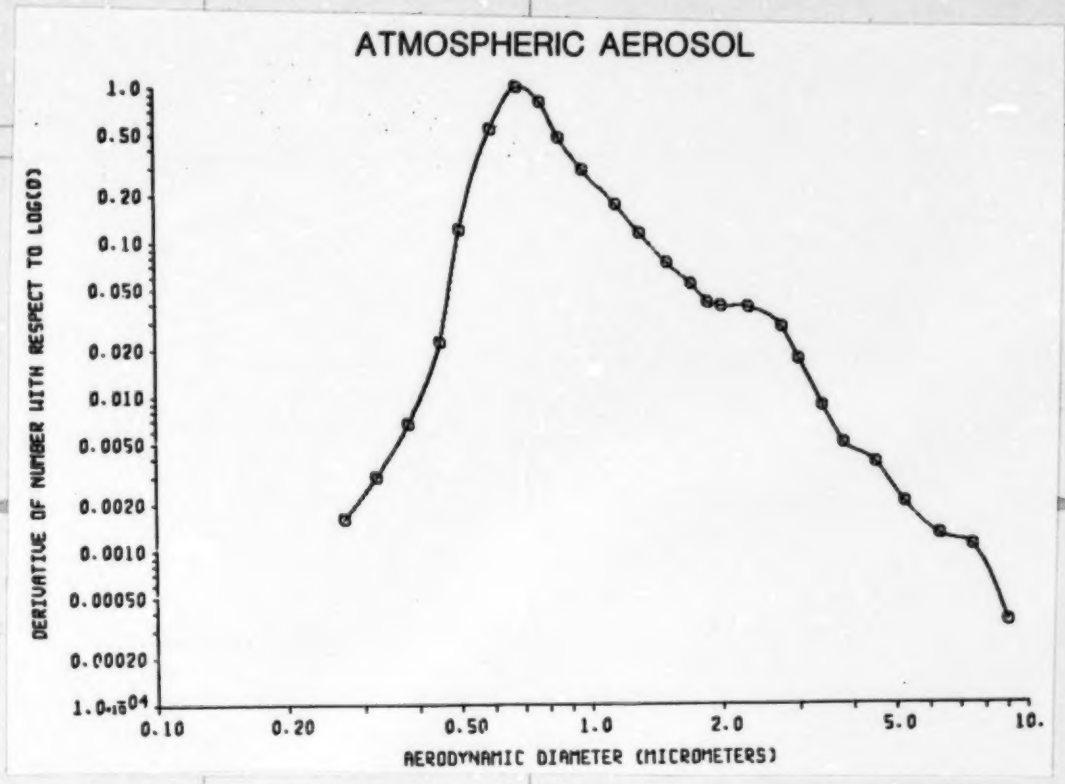

Figure 13. Size distribution of atmospheric aerosol as determined by the SPART analyzer, using $Q(d_a) = 0.01$ for the entire range.

Figure 14 shows size distributions [$dN/d(\log d_a)$] of a therapeutic aerosol at 37°C at two relative humidities (RH = 35 and 98 percent). The test aerosol was introduced into a 200-liter capacity chamber which was maintained at 37°C $\pm$ 0.2. The relative humidity varied from 35 to 98 percent. The sample aerosol was then drawn from the chamber into the SPART analyzer. The growth of aerosol particles at a high humidity is demonstrated by the results shown in Figure 14, indicating the possible use of the analyzer for studies of aerosol growth and decay.

The experimental data indicate that the SPART analyzer, in common with other recently developed instruments,[16,17] can measure aerodynamic diameters of individual particles in real time. A new type of SPART analyzer that uses an electric rather than an acoustic field has also been developed.[18]

BEGIN LAST LINE OF TEXT
3/8"
BOTTOM OF IMAGE AREA OUTSIDE DIMENSION FOR TABLES AND ILLUSTRATIONS

PAGE NUMBER
EPA Form 2350-4 (4-80)
(PREVIOUSLY CIN: EPA FORM 287)
☆ U.S. GOVERNMENT PRINTING OFFICE 1980-660-609
TYPING GUIDE SHEET

BEGIN FIRST LINE OF TEXT HERE
CENTER OF PAGE
TOP OF IMAGE AREA
DROPPED HEAD; BEGIN SECTIONS HERE

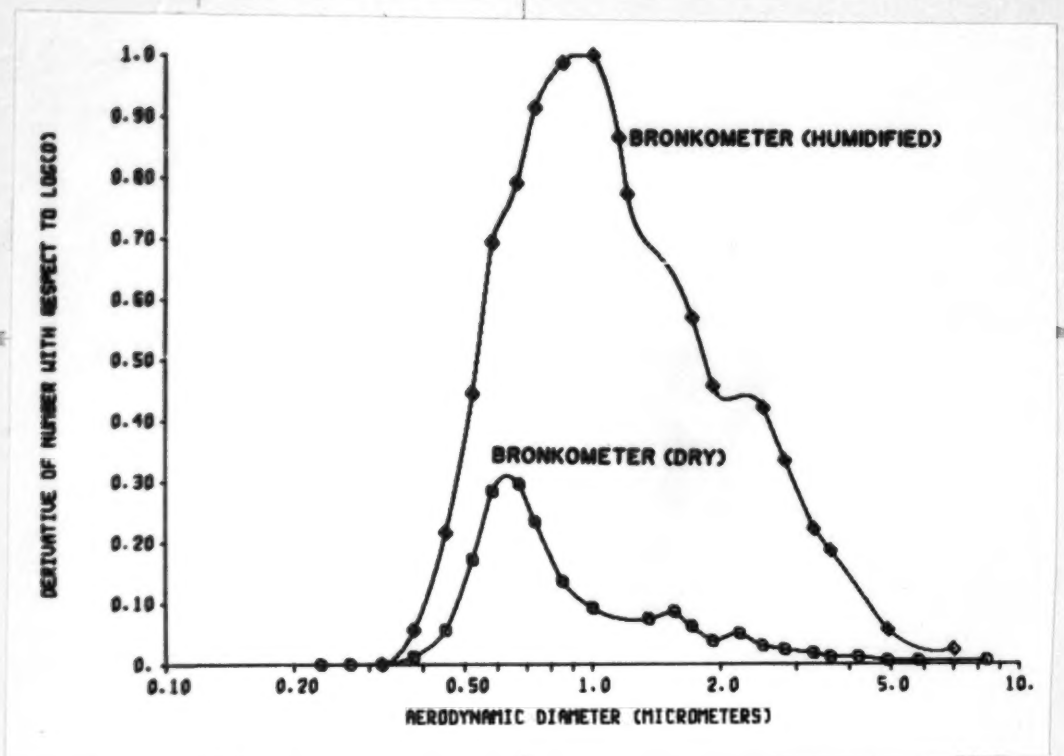

Figure 14. Growth of Bronkometer aerosol as measured by the SPART analyzer. The aerosol was generated by a metered-dose medical aerosol dispenser and was analyzed at 35 and 98 percent relative humidity while being maintained at 37°C. The value of $Q(d_a)$ used was 0.01 for the entire range.

BEGIN LAST LINE OF TEXT
BOTTOM OF IMAGE AREA; OUTSIDE DIMENSION FOR TABLES AND ILLUSTRATIONS
3/8"

EPA Form 2350-4 (4-80)
(PREVIOUSLY CIN, EPA FORM 237)
☆ U.S. GOVERNMENT PRINTING OFFICE 1980-680-639
TYPING GUIDE SHEET

BEGIN FIRST LINE OF TEXT HERE
CENTER OF PAGE
TOP OF IMAGE AREA
DROPPED HEAD; BEGIN SECTIONS HERE

REFERENCES

1. May, K. R., The Cascade Impactor: An Instrument for Sampling Coarse Aerosols, J. Sci. Instrum. 22:187-195, 1945.

2. Marple, V. A. and K. Willeke, Inertial Impactors: Theory, Design and Use. Fine Particles: Aerosol Generation, Measurement, Sampling, and Analysis, B. Y. Liu, Ed., Academic Press, Inc., New York, New York, 1976. pp. 412-446.

3. Fuchs, N. A., The Mechanics of Aerosols, Pergamon, New York, 1964. pp 77.

4. Mercer, T. T., Aerosol Technology in Hazard Evaluation, Academic, New York, 1973.

5. Beranek, L. L., Acoustics, McGraw-Hill, New York, New York, 1954. p. 286.

6. Durst, F., A. Melling, and J. H. Whitelaw, Principles and Practice of Laser-Doppler Anemometry. Academic, New York, New York, 1976.

7. Mazumder, M. K., Appl. Phys. Lett. 16, 1970. p. 462.

8. Mazumder, M. K., and K. J. Kirsch, Rev. Sci. Instrum. 48, 1977. p. 622.

9. Willeke, K., and B. Y. H. Liu, Single Particle Optical Counter: Principle and Application. Fine Particles: Aerosol Generation, Measurement, Sampling, and Analysis (Edited by Liu, B. Y. U.), Academic, New York, New York, 1976. p. 697.

10. Liu, B. Y. H., Standardization and Calibration of Aerosol Instruments. Fine Particles: Aerosol Generation, Measurement, Sampling, and Analysis (Edited by Liu, B. Y. H.), Academic, New York, New York, 1976. p. 40.

11. Mazumder, M. K., R. E. Ware, J. D. Wilson, R. G. Renninger, F. C. Hiller, P. C. McLeod, R. W. Raible, and M. K. Testerman, J. Aerosol Sci. 10:561, 1979.

6-1/2"
BEGIN LAST LINE OF TEXT
3/8"
BOTTOM OF IMAGE AREA; OUTSIDE DIMENSION FOR TABLES AND ILLUSTRATIONS

EPA Form 2350-4 (4-80)
(PREVIOUSLY CIN, EPA FORM 2371)
☆ U.S. GOVERNMENT PRINTING OFFICE 1980-660-639
TYPING GUIDE SHEET

BEGIN FIRST LINE OF TEXT HERE
CENTER OF PAGE
TOP OF IMAGE AREA

12. Husar, R. B., Recent Developments in in situ Size Spectrum Measurements of Submicron Aerosols, Instrumentation for Monitoring Air Quality, ASTM STP 555, Am. Soc. for Testing and Materials, 1974. pp. 157-192.

DROPPED HEAD; BEGIN SECTIONS HERE

13. Lewis, C. W., and P. J. Lamothe, J. Aerosol Sci. 9:391, 1978.

14. Hiller, C., M. K. Mazumder, D. Wilson, and R. Bone, Am. Rev. Respir. Dis. 118, 1978. p. 311.

15. Hiller, C., M. K. Mazumder, J. D. Wilson, R. C. Bone, Clinical Research 27:3, 399A, 1979.

16. Wilson, J. C. and B. Y. H. Liu, J. Aerosol Sci. 11:139, 1980.

17. Russo, A. J., L. E. Hackett, and R. H. Croll, Rev. Sci. Instrum. 50, 1391-1395, 1979.

6-1/2"

18. Renninger, R. G., M. K. Mazumder and M. K. Testerman, Rev. Sci. Instrum. 52, 242-246, 1981.

9-1/8"

BEGIN LAST LINE OF TEXT
BOTTOM OF IMAGE AREA OUTSIDE DIMENSION FOR TABLES AND ILLUSTRATIONS
3/8"

EPA Form 2350-4 (4-80)
(PREVIOUSLY CIN. EPA FORM 287)
☆ U.S. GOVERNMENT PRINTING OFFICE 1980-660-639
TYPING GUIDE SHEET